REVIEW

Current and future applications of ultrasound imaging in peripheral nerve disorders

Antonia S Carroll, Neil G Simon

ORCID number: Antonia S Carroll (0000-0002-1738-9580); Neil G Simon (0000-0003-1784-8238).

Conflict-of-interest statement: There is no conflict of interest associated with any of the senior author or other coauthors contributed their efforts in this manuscript.

Antonia S Carroll, Brain and Mind Research Centre, University of Sydney, Camperdown 2050, NSW, Australia

Antonia S Carroll, Department of Neurology, Westmead Hospital, University of Sydney, Westmead 2145, NSW, Australia

Antonia S Carroll, Department of Neurology, St Vincent's Hospital, Sydney, Darlinghurst 2010, NSW, Australia

Neil G Simon, Northern Clinical School, University of Sydney, Frenchs Forest 2086, NSW, Australia

Corresponding author: Neil G Simon, FRACP, MBBS, PhD, Doctor, Senior Lecturer, Northern Clinical School, The University of Sydney, Northern Beaches Hospital, Suite 14A, Frenchs Forest 2086, NSW, Australia. neil@nbneuro.com.au

Abstract

Neuromuscular ultrasound (NMUS) is a rapidly evolving technique used in neuromuscular medicine to provide complimentary information to standard electrodiagnostic studies. NMUS provides a dynamic, real time assessment of anatomy which can alter both diagnostic and management pathways in peripheral nerve disorders. This review describes the current and future techniques used in NMUS and details the applications and developments in the diagnosis and monitoring of compressive, hereditary, immune-mediated and axonal peripheral nerve disorders, and motor neuron diseases. Technological advances have allowed the increased utilisation of ultrasound for management of peripheral nerve disorders; however, several practical considerations need to be taken into account to facilitate the widespread uptake of this technique.

Key words: Neuromuscular ultrasound; Peripheral neuropathy; Polyneuropathy; Entrapment neuropathy; Immune-mediated neuropathy; Hereditary neuropathy

Core tip: Neuromuscular ultrasound is now an extension of the clinical examination, providing complimentary structural information to standard electrodiagnostics. Typical ultrasonographic patterns can assist to distinguish neuropathies of different aetiologies and is increasingly used as a non-invasive biomarker to monitor treatment effect.

INTRODUCTION

Ultrasound (US) technology was initially developed for medical use in the 1940s, where A-mode linear recordings displayed alterations in echointensity as amplitude. Here, a single pulse of US is transmitted to the tissue, resulting in a one-dimensional linear representation of reflected US beams as a function of depth. Further technological advances allowed for the development of B-mode or 2D-mode, still used today, where multiple linear data channels are superimposed to create an image where amplitude is expressed as brightness. However, US was not applied to peripheral nerves prior to the 1980s[1,2] due to inadequate image resolution and difficulty discerning nerve from surrounding tissues of similar echogenicity[3]. The first report of the diagnostic utility of peripheral nerve US, used to detect carpal tunnel syndrome (CTS), was published in 1991[4]. Since then, US technology has continued to evolve with the development of broadband high-frequency linear-array transducers, Doppler technology and post-processing software programs, all of which have increased the ability of US to identify anatomic and structural abnormalities in nerves.

Today US imaging is increasingly and commonly used as an adjunct to clinical and neurophysiological studies in the evaluation of neuromuscular diseases, so called neuromuscular ultrasound (NMUS). Advantages of NMUS include being a non-invasive, painless, economical, portable and fast test, whilst allowing a high resolution, dynamic assessment of the complete nerve in real-time. Thus, NMUS is considered an ideal screening, diagnostic and monitoring tool. An alternative imaging modality is Magnetic resonance (MR) neurography which provides exceptional three-dimensional images of neural anatomy as well as functional characteristics with the advent of tractography and diffusion tensor imaging[5,6]. Furthermore quantitative techniques, such as the fat fraction of muscles and nerve size, can be used to monitor disease progression, and may be beneficial as biomarkers in future clinical trials[7]. However, MR Neurography is expensive, time-consuming, poorly tolerated in children and claustrophobic individuals, limited in availability and, in clinical practice, restricted to the pre-specified region. Compared to MR Neurography, NMUS provides improved spatial resolution with extremely small nerves being amenable to investigation; however, deep neural structures, such as the lumbosacral plexus and proximal sciatic nerve, or those deep to osseous structures are unable to be imaged. Hence there is an ongoing complementary role for both NMUS and MR Neurography; however, the use of each imaging modality needs to be tailored to the correct clinical situation.

CURRENT AND FUTURE APPROACHES AND TECHNIQUES

B-mode

NMUS is predominantly performed in B- or 2D-Mode using a linear array transducer with an upper frequency of 15-18 MHz. Anatomy is assessed, along with the shape, echogenicity and cross-sectional area (CSA) of the nerve. Typically, a distal to proximal approach is followed to identify any abnormality along the course of the nerve. Structures should be assessed in two orthogonal planes, usually with cross-sectional (Figure 1A) and longitudinal (Figure 1B) views, and these images should be saved as documentation and to examine temporal trends. Comparison with the contralateral nerve is clinically useful for the evaluation of unilateral diseases. The mobility of the nerve, particularly around joints, can also be dynamically assessed, if relevant, such as the ulnar nerve at the elbow and median nerve at the wrist. In addition, muscles can be evaluated for neurogenic or myopathic changes. In neurogenic conditions fasciculations, atrophy and a patchy increase in echogenicity is typically demonstrated[8,9]. In contrast, in myopathic conditions homogenously increased echogenicity and increased Doppler signal is observed[8,9]. The specific US features of different muscle disorders is beyond the scope of this review and readers are directed to specific reviews on this topic[10-13].
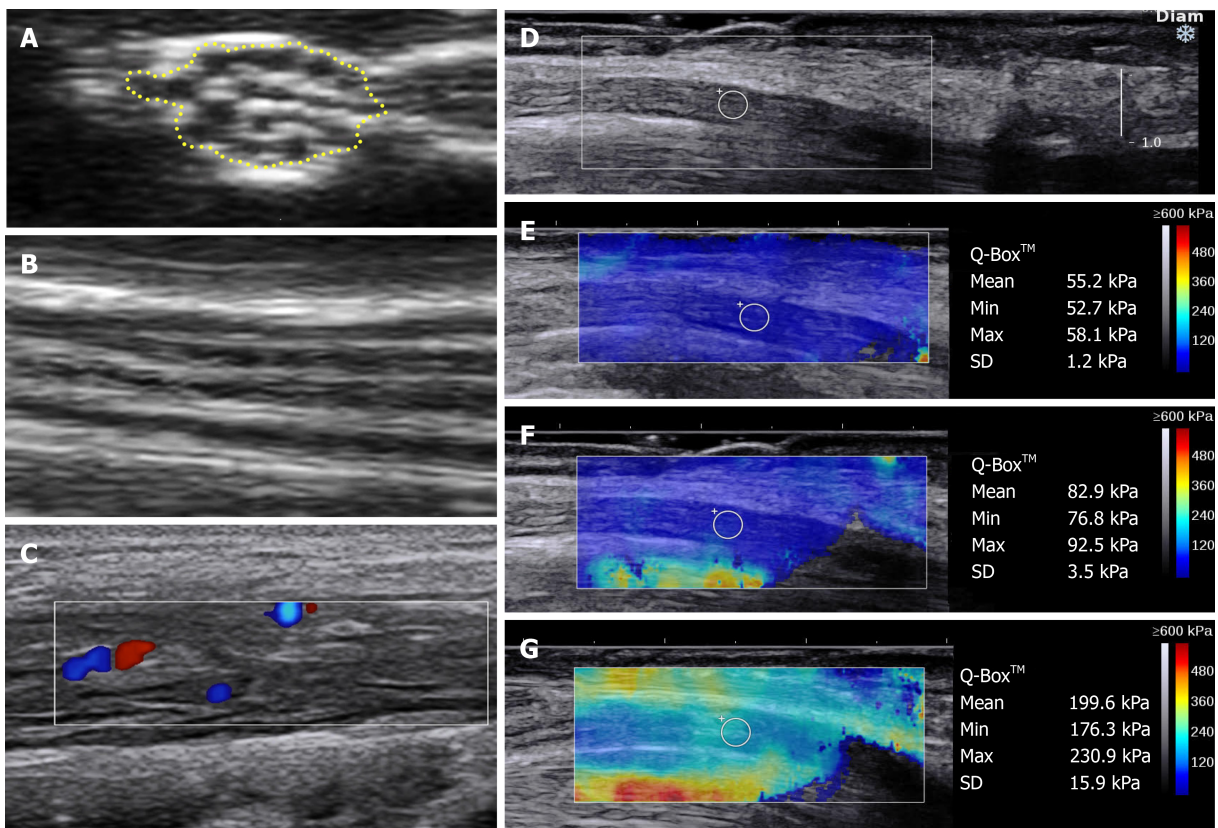
Figure 1 Approaches and techniques used in neuromuscular ultrasound. A and B: Normal nerve ultrasound appearances of the median nerve in the forearm in B-mode. A: Cross-sectional area traced within the hyperechoic rim; B: Longitudinal view demonstrating the normal linear fascicular pattern; C: Doppler signal in the tibial nerve of a patient with hypertrophic perineuritis; D-G: Sheer wave elastography in carpal tunnel syndrome; D: Longitudinal B-mode image of the median nerve at the carpal tunnel above the lunate bone, a typical location for elastography measurements; E: Elastography values in a normal wrist; F: increased median nerve stiffness in mild carpal tunnel syndrome; G: further increased median nerve stiffness in severe carpal tunnel syndrome. D-G: Citation: Wee TC, Simon NG. Ultrasound elastography for the evaluation of peripheral nerves: A systematic review. *Muscle Nerve* 2019; 60: 501-512. Copyright© The Authors 2020. Published by John Wiley and Sons.

CSA: Nerve size is measured using CSA, measured in mm², which is traced within the hyperechoic epineurial rim of the nerve with the transducer perpendicular to the nerve. Care must be taken to measure a true CSA as CSA is frequently overestimated when using an oblique view of the nerve. CSA is the most commonly used measure to quantify abnormalities in nerve diseases, due to its reproducibility and high inter- and intra-assessor reliability[14]. Normative reference values are available for the main limb nerves, the brachial plexus and cervical roots[15-18]. Physical characteristics, such as age, gender, height and body-mass index, and temperature have been identified, in some publications, to alter nerve size[15,16,19], therefore, ideally standardised conditions should be used for all tests, and local normative values should be collected.

Echogenicity: Echogenicity of a peripheral nerve is commonly described and typically varies in normal individuals along the length of a nerve, with the proximal segments appearing more hypoechoic than the distal segments[20]. The echotexture of the nerve can be semi-quantitatively evaluated by assessing the mean grey scale value of a selected image, or can be quantified by post-processing software using thresholding techniques to determine the hypoechoic fraction and density of the nerve[21,22]. Of note quantitative measures of echotexture are not comparable and vary with US systems, settings and processing software, which limits its utility as a potential disease biomarker. Figure 2 demonstrates qualitative alterations in nerve echotexture in different pathological conditions.

Ultra-high frequency B-mode: Since the development of US, continual modification of US probes and signal processing has resulted in improved image resolution and quantification. In 2016 the first ultra-high frequency transducer (Vevo MD ultrasound device, FujiFilm Visual Sonics, Toronto, Ontario, Canada), with a maximum frequency of 70 MHz, was approved for clinical use by the Food and Drug Administration (FDA) allowing extremely high-resolution imaging of neural and other structures. However, this dramatic enhancement of resolution to 30 μm, comes
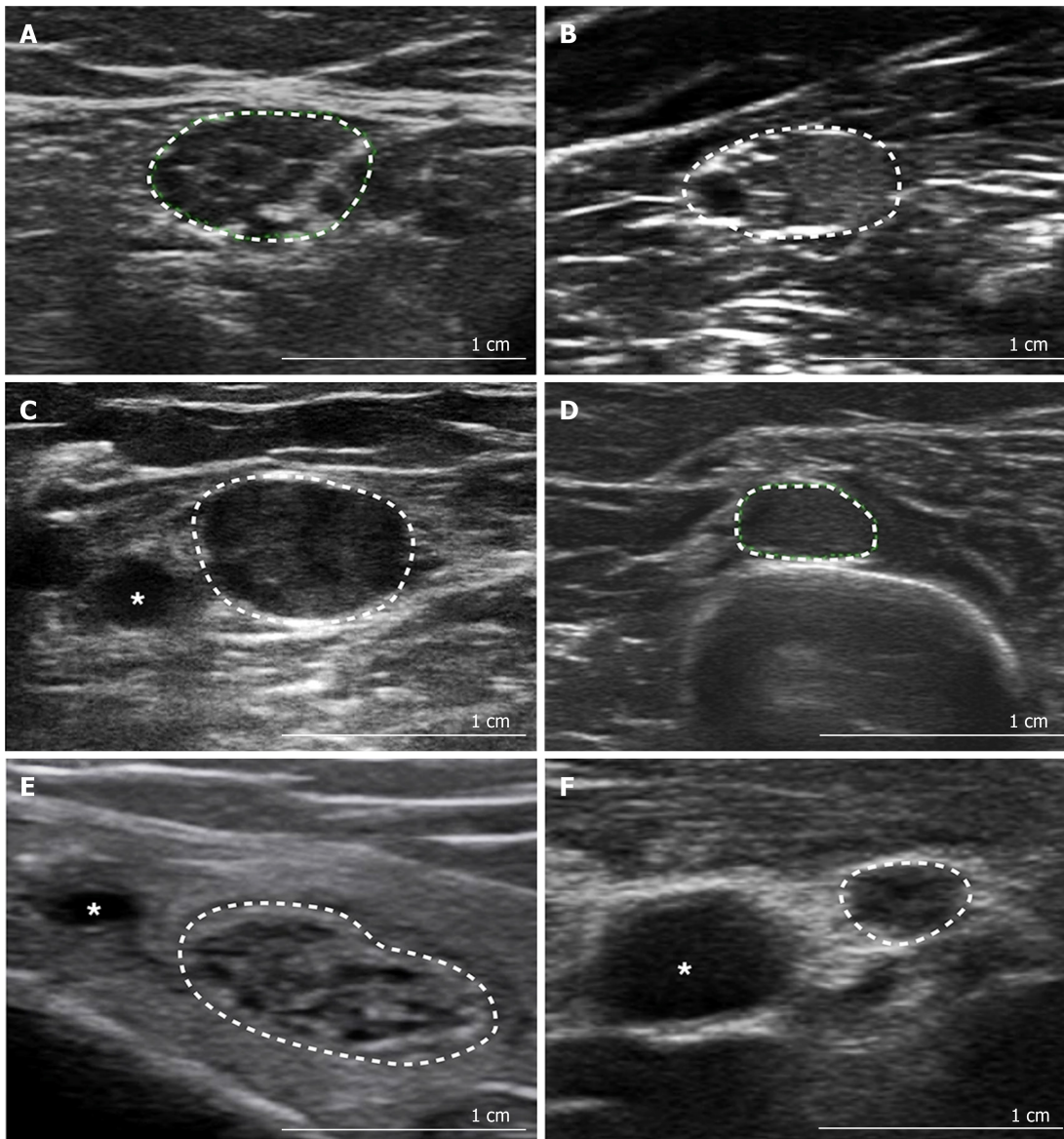
Figure 2 Patterns of neuromuscular ultrasound in peripheral neuropathy. A: Non-homogenously enlarged, hypoechoic fascicles in Charcot Marie Tooth disease type 1A [tibial nerve at the ankle, cross-sectional area (CSA) 49 mm^2]; B: Hyperechoic and hypoechoic fascicles in chronic inflammatory demyelinating polyradiculoneuropathy (CIDP) (median nerve in the forearm, CSA 65 mm^2); C: Interruption of the fascicular structure in multifocal acquired demyelinating sensory and motor neuropathy (median nerve at the elbow, CSA 91 mm^2); D: Enlarged CSA, in a region normally associated with mono- or oligo-fascicular appearances, in a patient with CIDP (radial nerve at the spiral groove, CSA 27 mm^2); E: Enlarged CSA, with reasonably normal fascicular architecture, due to increased perineurial connective tissue in hypertrophic neuropathy (tibial nerve at the ankle, CSA 95 mm^2); F: Normal CSA with distorted fascicular architecture in amyloid neuropathy (median nerve at midpoint of the arm, CSA 8 mm^2). Citation: Gallardo E, Noto Y, Simon NG. Ultrasound in the diagnosis of peripheral neuropathy: structure meets function in the neuromuscular clinic. *J Neurol Neurosurg Psychiatry* 2015; 86: 1066-1074. Copyright© The Authors 2020 with permission from BMJ Publishing Group Ltd.

at the expense of penetration depth. Specifically, the 70 MHz probes are only able to image superficial structures, up to a maximum of 3 cm in depth. However, despite this limitation, the use of ultra-high frequency US allows significant insights into the internal neural structures providing detailed data on the size, number and density of fascicles, echogenicity and intraneural vascularisation. To date this technology has been used to accumulate normative data in median and ulnar nerves and to evaluate chronic inflammatory demyelinating polyradiculoneuropathy (CIDP) and spinal muscular atrophy (SMA)[23-26].

Fascicular US: Improvements in US resolution has facilitated further in-depth analysis of smaller neural structures, such as individual nerve fascicles. Variation of individual nerve fascicle size will likely provide pathological insights in peripheral neuropathies, nerve tumours and nerve trauma. In the context of CSA enlargement, nerve fascicles are often enlarged; however, this is not always homogenous[27]. For example, fascicular size has been evaluated in Charcot Marie Tooth disease type 1A

(CMT1A), revealing significant diffuse fascicular enlargement across nerves, but interestingly, non-homogenous enlargement across the fascicles of an individual nerve[28]. Similar, but more pronounced, variability in fascicular enlargement has been seen in CIDP, multifocal motor neuropathy (MMN) and vasculitis, with regional and differential enlargements observed[13,25,28,29]. However, the interpretation of fascicular size is complex, as the calibre of the fascicles can vary between different nerves, the same nerve in different locations, and between individuals. For example, the brachial plexus trunks are typically comprised of two large fascicles, whereas the median nerve in the forearm is comprised of a multitude of smaller fascicles, up to 30 in one study[23]. As a result, a standardised approach and normative values are required for future utility of this approach.

Recently normal values have been published for the upper limit of normal fascicular sizes in the median, ulnar and peroneal nerves[28]. In addition a fascicle pattern grading system was proposed, using the summed proportion of enlarged fascicles in the median, ulnar and peroneal nerves and the proportion of enlarged fascicles within the individual nerve, to distinguish between inherited and acquired neuropathies[28]. Further large prospective studies using various US probes and assessing several anatomical locations will be required to validate the proposed fascicle pattern grading system, provide further normative data and solidify the use of fascicle size as a monitoring or diagnostic biomarker.

Doppler US

B-mode can be used with Colour or Power Doppler to quantify blood flow (Figure 1C). Blood flow, both intraneural or epineural, is not able to be detected in normal nerves using current non-contrast imaging[30]. Increased blood flow, described qualitatively or quantitatively, can be seen in acquired inflammatory neuropathies, neurolymphomatosis or in nerve entrapment[31-38], and is best evaluated with Power Doppler which is more sensitive for low flow states, such as is found intraneurally[39]. Autonomic activation, by provocative manoeuvres, exercise, or electrical stimuli, can alter neural blood flow, as can tremor and abnormal arterial anatomy, both congenital and iatrogenic, hence, patient selection and positioning is necessary to ensure the generalisability of results[40].

Currently used quantitative measures are surrogates for intraneural blood flow including manual counts of Doppler signals or the analysis of Doppler waveforms to assess the velocity of blood flow. These measures more correctly indicate hypervascularity, rather than a definitive increase in blood volume within the nerve, and, due to the slow flow within nerves, likely underestimate intraneural blood flow due to detection thresholds of flow velocity[41]. Recently additional techniques have been used to more accurately assess intraneural blood flow including contrast enhanced ultrasound (CEUS) and measurement of maximum perfusion intensity (MPI)[41,42].

CEUS: Novel approaches to measuring intraneural blood flow have been recently published in attempts to improve the accuracy and precision of vascularity measures and better understand pathophysiology and treatment response in neuropathies. Two pilot studies of CEUS in normal median nerves, were able to safely and reproducibly detect microvascularity in asymptomatic cohorts[42,43]. CEUS has been subsequently used to evaluate animal models with CTS and sciatic nerve crush injuries, and in humans with CTS and for intra-operative differentiation of peripheral nerve tumours[44-47]. High-resolution CEUS has allowed the quantification of previously undetectable low volume intraneural blood flow; however, further studies are required to evaluate its use in the assessment of disease severity and prognosis in peripheral nerve diseases. To date studies have been limited due to FDA restrictions on the use of contrast agents, despite its approval and safety record for use in echocardiography[48].

MPI: Similar methods have been proposed to quantify intraneural blood flow without using contrast, including the measurement of MPI. This uses a semiautomated, validated perfusion measurement software, such as PixelFlux (Chameleon Software, Munster, Germany), to measure the MPI by quantifying blood flow using the intensity of colour hues of the pixels within a specified region of interest in an uploaded Doppler US video file[41]. An initial study identified improved reliability of MPI compared to previous semi-quantitative vessel scores in CTS, and correlations with neurophysiologically determined CTS severity and nerve CSA[41]. MPI has subsequently been applied in diabetic neuropathy and end-stage kidney disease, finding correlations between intraneural blood flow measurements, nerve size, symptomatology and neuropathy severity scores[49,50]. Interestingly, in the haemodialysis cohort, blood flow measurements were significantly improved after

dialysis, suggesting that this measure may have future utility as a biomarker of both disease severity and treatment response[50].

Elastography

US Elastography is an additional functional technique which has garnered increasing interest as a potential prognostic and monitoring biomarker in neuromuscular diseases. Elastography non-invasively measures the stiffness of tissues, which reflects underlying pathological changes in tissue composition and architecture. Stiffness tends to increase in peripheral neuropathy of all causes, consistent with the replacement of compliant myelin with various less-compliant connective and other tissues[51]. Strain and shear-wave elastography (SWE) are the two major techniques, differing in measurement methodology.

Strain elastography: Strain elastography measures stiffness by recording the displacement of a tissue by either a manual compression or by physiologic tissue movement, such as cardiorespiratory pulsations. The latter method, specifically known as ambient strain elastography (ASE) is preferred for neuromuscular evaluation as it is more reproducible and reliable for clinical practice, than manual compression techniques where the quantification and standardisation of force is challenging[52].

SWE: Alternatively, SWE uses a standardised high-intensity acoustic or vibration pulse to cause tissue displacement generating a quantitative measure of stiffness (Figure 1D-G), with similarly reproducible and reliable findings to ASE[51].

The output of these different elastography modalities is not comparable and at present, despite the benefit of quantitative results with SWE, the choice of technique is most frequently determined by the availability of elastography modules and local expertise. US elastography techniques have predominantly investigated the median nerve at the wrist, to date, finding elevated stiffness in CTS compared with control wrists, and in some studies, severity of CTS correlating with increasing nerve stiffness (Figure 1E-G)[53-59]. However, further studies evaluating elastography as a diagnostic and monitoring biomarker are required to cement its use in clinical practice.

Applications

NMUS also allows for the improved evaluation of children and phobic individuals who tolerate electrodiagnostics (EDX) poorly, as well as access to technically challenging or inaccessible sites. The diaphragm, for example, is technically difficult to assess, with nerve conduction studies being unreliable and affected by body habitus, and electromyography (EMG) risky in the context of critical respiratory insufficiency and the potential to precipitate a pneumothorax[60]. The diaphragm is easy to US and demonstrates both acute or chronic changes characterised by the degree of movement and alterations in thickness during the respiratory cycle. The ratio of inspiratory-expiratory thickness has a sensitivity of 93% and specificity of 100% for neuromuscular diaphragmatic dysfunction[61]. US can also be used in this setting to reduce risk by guiding EMG, and as an alternative to radiological respiratory function tests, such as the "sniff test"[62].

NORMAL SONOGRAPHIC APPEARANCE OF PERIPHERAL NERVE

Ultrasonographic appearances of normal peripheral nerve parallel the anatomy of the nerve at both a micro- and macroscopic level[1]. In cross-section nerves display a "honeycomb" appearance reflecting the hypoechoic fascicles surrounded by hyperechoic epineurium and perineurium (Figure 1A). In longitudinal view a nerve appearance is described as a "train-track", with a linear hypoechoic fascicle with hyperechoic edges (Figure 1B). Proximal segments of nerve, such as the roots and plexus, appear more hypoechoic due to reduced connective tissue composition and increased fascicle density[20,63]. As a normal nerve progresses distally the CSA tapers[15]. This finding is more pronounced in the lower limb nerves than in the upper limbs. In healthy individuals, nerves can have focal enlargements closer to entrapment sites[15].

The hyperechoic appearance of the epineurium is caused by the high impedance of the densely packed connective tissue. This characteristic finding is useful to differentiate nerves from other structures. Anisotropy, an artefact generated by tilting the probe, can also be used to distinguish nerves. Nerves typically have low anisotropy, meaning that there is minimal alteration in echogenicity with change of the transducer angle. This low anisotropy aids to distinguish nerve from tendons and muscle, which have high anisotropy, changing from hyperechoic to hypoechoic

appearance with movement of the transducer angle from perpendicular to parallel. Vessels can be differentiated from nerve by the identification of pulsatile movement, collapsibility under pressure or flow on Doppler.

US APPEARANCES IN PERIPHERAL NERVE DISORDERS

Typical morphological changes in the nerve are seen after nerve injury of many causes, including enlargement in nerve size and reduced echogenicity. The latter is proposed to be due to intraneural oedema caused by thickening of connective tissues, increased vascular leak and/or vascular proliferation[3,64]. Injury to the nerve also typically cause alterations in fascicular architecture and intraneural blood flow. In the following sections the specific US findings observed in entrapment, hereditary, immune-mediated and axonal neuropathies, and motor neuron diseases will be discussed. Figure 2A-F outlines the typical sonographic patterns identified on NMUS in various polyneuropathies. Figure 3 provides an overview of the degree and distribution of nerve enlargement in inherited and acquired polyneuropathies.

Peripheral nerve entrapment

In compressive neuropathies localised enlargement, just proximal to the site of compression, decreased echogenicity, loss of the internal fascicular structure and increased blood flow can all be commonly observed[3,65]. However, a maximum point of enlargement should be identified along the course proximal and distal to the site of compression as enlargement can be present distal to the entrapment site, and nerve mobility may alter the positioning of such enlargements[66]. The entrapment site may display an hour-glass or spindle-shaped appearance in longitudinal views[66]. Strictures, ganglion cysts, tumours, thrombosed arteries and other extrinsically or intrinsically compressive lesions can be identified by US as the cause of symptomatology, and hence can drastically alter the management paradigm. In one study of mononeuropathies the diagnostic or management trajectory was altered by peripheral nerve US in over 42% of cases[67]. The use of peripheral nerve US assists to identify early or neurophysiologically normal disease, localises the lesion, and can identify the cause of compression, and hence complements traditional EDX techniques.

The earliest identifiable ultrasonographic sign of compression is reduced echogenicity within the nerve followed by nerve enlargement. Pressure of the US probe over the compressed section of nerve can reproduce clinical symptoms, a so called "Sonographic Tinel" sign. With ongoing progression of entrapment denervation features of the distal muscles can develop including increased muscle echogenicity and fasciculation, and later atrophy. The characteristic ultrasonographic findings seen in specific compressive neuropathies is summarised in Table 1.

Hereditary neuropathies

Peripheral nerve US has been used as a diagnostic tool in Charcot-Marie-Tooth disease (CMT), Hereditary neuropathy with liability to pressure palsies (HNPP) and more recently in hereditary transthyretin (ATTRv) amyloidosis and sensory neuropathies and neuronopathies associated with cerebellar ataxia, neuropathy, and vestibular areflexia syndrome (CANVAS), spinocerebellar ataxias (SCA) and Freidrich's ataxia (FRDA).

CMT: An early study using a 7.5 MHz linear array probe to investigate the role of peripheral nerve US in CMT suggested that the technique had limited utility in distinguishing CMT from healthy subjects[148]. The diameter and echogenicity of nerves, but not the CSA, was evaluated and found not to differ from healthy controls, and the increased echogenicity of adjacent muscles made neural structures more difficult to assess in the CMT cohort. However, with the advent of higher frequency probes, which have improved US resolution, characteristic findings have been identified in subtypes of CMT.

CMT1A: In CMT1A, the most common demyelinating form of CMT caused by a duplication the peripheral myelin protein 22 gene, the CSA of proximal and distal nerves, plexuses and roots are typically found to be diffusely, uniformly and symmetrically enlarged, analogous to the typical uniformity seen in nerve conduction velocities (Figure 2A)[3,149-151]. In general the CSA enlargement in CMT1A is greater than twice that of healthy controls (Figure 3D)[152]. Furthermore, the CSA enlargement has been found to parallel clinical and electrodiagnostic parameters in CMT. Specifically, the CSA of the median nerve correlates with a CMT severity rating score, the CMT neuropathy score, and greater CSA correlates with reduced motor
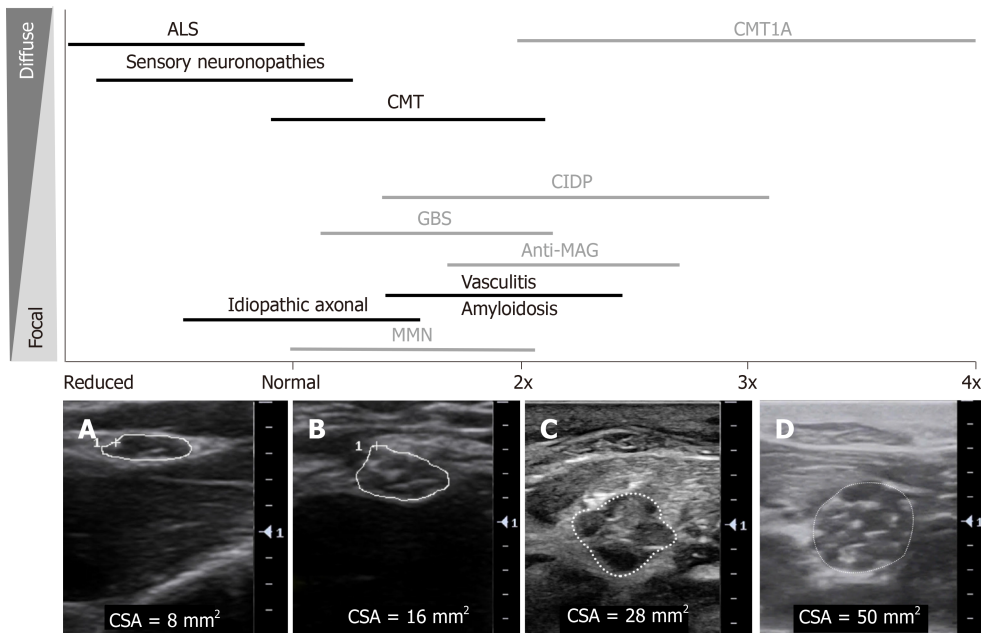
Figure 3 An overview of sonographic findings in inherited and acquired polyneuropathies: degree and distribution of nerve enlargement. Black: Axonal neuropathies, Grey: Demyelinating neuropathies. Cross-sectional area (CSA) shown in: A: Median nerve at the elbow in a patient with amyotrophic lateral sclerosis, CSA 8 mm²; B: Median nerve at the elbow in a healthy control, CSA 16 mm²; C: Median nerve in the forearm in a patient with chronic inflammatory demyelinating polyradiculoneuropathy, CSA 28 mm², with heterogeneously enlarged, hypoechoic fascicles; D: Median nerve in the forearm in a patient with Charcot Marie Tooth disease type 1A, CSA 50 mm², with more homogenously enlarged, hypoechoic fascicles. ALS: Amyotrophic lateral sclerosis; CMT1A: Charcot Marie Tooth disease type 1A; CMT: Charcot-Marie-Tooth disease; CIDP: Chronic inflammatory demyelinating polyradiculoneuropathy; GBS: Guillain-Barre syndrome; MAG: Myelin-associated glycoprotein; MMN: Multifocal motor neuropathy; CSA: Cross-sectional area.

conduction velocities and compound muscle action potential amplitudes[153]. Thus, suggesting that US findings reflect both the physiological function and disease severity in CMT1A.

However, variability has been identified in the CSA of the sural nerve in patients with CMT1A, with studies identifying either no, or significant, differences when compared with healthy controls, which may reflect differing techniques for CSA measurement[153,154]. In addition, in CMT1A there is diffuse fascicular enlargement across nerves; however, within an individual nerve there is variability in the extent of fascicular enlargement[27,28]. Nerves are reported to be more hypoechogenic and display no increase in vascularity[151].

CMT1A can be distinguished from other axonal and intermediate subtypes of CMT, including CMT2 and CMTX1, by a greater CSA or fascicular diameter of the median nerve and minimal variation between entrapment and non-entrapment sites[27,155]. In addition, the CSA of the median, ulnar and peroneal nerves has been found to be significantly greater in CMT1A than in other demyelinating forms of CMT, including CMT1B, demyelinating CMTX and CMT4C; however, more overlap in CSA is observed[149].

CMT1B: In demyelinating CMT1B, due to mutations in Myelin Protein Zero (MPZ), the median and vagus nerve CSAs were enlarged compared to normal individuals[156]. However, across the spectrum of CMT caused by mutations in MPZ, which can cause a demyelinating (CMT1B), axonal (CMT2I/2J) or intermediate (CMTDID) phenotype[157], the CSA of only the demyelinating subgroup was found to be enlarged in the median and ulnar nerves, in particular at proximal nerve sites[158]. Similarly the C5 nerve root CSA was enlarged in both the demyelinating and intermediate groups[158]. NMUS of lower limb nerves in CMT1B have consistently revealed reduced calibre nerves, with considerable overlap between the demyelinating, axonal and intermediate subgroups, thought indicative of a floor-effect due to length dependent axonal losses[156,158]. Taken together, this suggests that peripheral nerve US comparing distal to proximal segments of upper limb nerves may be most useful to differentiate the subtypes of CMT associated with MPZ mutations, and that intranerve CSA variability could assist to distinguish CMT1B from CMT1A.

CMT1X: CMT1X, the second most common form of CMT, is an X-linked intermediate CMT associated with mutations in gap junction-associated protein B1[157]. Initial

Table 1 Characteristic ultrasound findings in entrapment neuropathies

	CSA	Echogenicity	Vascularity	Other
Median neuropathy at the wrist – CTS	Increased CSA at the distal wrist crease[68]	Reduced median nerve echogenicity proximal to compression site both with[77,78] and without EDX abnormalities in 82.4%[79]	Increased median nerve vascularity, with[65] and without EDX abnormalities in 7.1%[79]	Reduced median nerve mobility (transverse and longitudinal) with[77,80,81] and without EDX abnormalities in 75%[79]
	Range ULN 8.5-12 mm^2[69-73]		In CTS confirmed on EDX:[65]	Reduced transverse sliding of the median nerve correlated with presence of CTS and severity of CTS[82,83]
	Using ULN of 8.5-10 mm^2 for the diagnosis of CTS[74]	Loss of fascicular architecture	Sensitivity 95%	Improved mobility post steroid injection[78]
	Sensitivity 65%-97%, Specificity 72.7%-98%, PPV 79%-97%		Specificity 71%	Increased Median nerve stiffness - seen with all elastography modalities[51]:
	WFR > 1.4[68]		PPV 94%	Correlates with severity[84,85]
	Comparing 12 cm proximal to the distal wrist crease		Improves post steroid injection[78]	Stiffness decreases after CTS release[86] and steroid injections[87]
	Sensitivity 100% (Specificity NA)			Identify anomalous anatomy:
	US parameters suggested for the presence of CTS with normal EDX[66]:			Bifid median nerve 5%-10%[88-90]
	CSA > 14 mm^2			Persistent median artery 0.5%-3.7%[88,90]
	WFR > 1.8			Anomalous muscles in the carpal tunnel[91]
	In CTS with a negative US at the distal wrist crease, 25% have CSA enlargement in the distal carpal tunnel.			
	Scanning the whole carpal tunnel increases sensitivity by 15%-20%[75,76]			
UNE	Increased CSA, maximal at medial epicondyle	Reduced nerve echogenicity and increased nerve hypoechoic fraction[22,98]	Intraneural vascularisation[100,101]	Ulnar nerve subluxation with elbow flexion in 14%-23.1%; dislocation across the medial epicondyle in 8.5%[94]
	ULN 8-11 mm^2, most commonly 10 mm^2[92-96]	Hypoechoic fraction increased distal and proximal to the medial epicondyle[98]	Present in 15%	Ulnar nerve dislocation and symptomatic UNE can be found in the context of negative EDX findings
	Using the following cut-off values for UNE:		Correlated with axonal loss, atrophy and increased CSA	Highest diagnostic yield is in patients with EDX abnormalities, but unable to localise - diagnosis confirmed by US in 86%[93]
	> 9 mm^2 - Sensitivity 84%, Specificity 80%[97]			Alternative locations for entrapment
	> 11 mm^2 - Sensitivity 95%, Specificity 71%[95]			Arcade of Struthers[102]
	Note: Maximal CSA may not be at the site of EDX abnormality[98]			Wrist[103]
	Increased ratio of nerve CSA at elbow compared with arm or forearm[95,96,98,99]			Identification of alternate aetiologies[104-112], *e.g.* trauma, brachial artery occlusion, scar tissue, haematoma, subdermal implants, venepuncture, ganglion cysts, anconeus epitrochlearis muscle
	Upper arm swelling ratio > 2.1[96]			Guide management[113,114]
	Max CSA/ Mid-upper arm CSA			Cubital tunnel – entrapment – benefits surgical decompression

	Sensitivity 60%, Specificity 74%			Epicondylar groove – external compression or stretching – no benefit from surgery
	Forearm swelling ratio > 2.3[96]			
	Max CSA/ Mid-forearm CSA			
	Sensitivity 65%, Specificity 79%, PPV 89.2%			
Radial neuropathy at the spiral groove or PIN	Increased CSA[16,66,115,116]: Radial nerve in spiral groove and antecubital fossa – ULN 9-10 mm²; Posterior interosseous nerve – ULN 1-2 mm²; Superficial radial nerve - ULN 1-3 mm²	Loss of echogenicity with PIN at level of maximal CSA[117]	Intraneural hypervascularity at site of compression[118]	Loss of fascicular structure with PIN at site of maximal CSA[117]; Provides additional information complementing EDX in 84%[116]
Common peroneal neuropathy at fibular head	Increased CSA at fibular head; ULN 8-14 mm², commonly 11 mm²[16,119-122]; Using the following cut-off values for the common peroneal nerve at the fibular head: > 8 mm² - Sensitivity 90%, Specificity 69%[120]; > 11.5 mm² - Sensitivity 89%, Specificity 99%[121]; Suggested cut-offs: 8 mm² if abnormal EDX[120]; 11 mm² for normal EDX[120]; CSA may be normal if conduction block, but no axonal loss, on EDX[123]	Loss of echogenicity at the site of maximal compression, with and without a normal CSA[121,124]	NA	Sensitivity for diagnosis[125]: 90% (95%CI, 79.7%- 97.3%); US localisation[120]: Fibular head 55%; Above fibular head 71%; Addition of US to EDX allowed for localisation in 88%, compared with 65.5% EDX alone[120]; Alternate aetiology[16,126,127]: Ganglion cysts (18% of cases) lipomas, scar tissue after knee surgery, abnormal biceps femoris anatomy; Guides requirement for surgical intervention[128]
LCFN - MP	Increased CSA at anterior superior iliac spine[129,130]; 4-5 mm²[129,130]; ULN 5 mm² – Sensitivity 95.7%, Specificity 95.5%, PPV 95.7%[130]; Increased nerve diameter 4 mm[129]	Intraneural hypoechogenicity[129]	NA	Anatomical variants in 20%[131]; LFC nerve closer to/lateral to the Anterior superior iliac spine in patients with idiopathic MP[132,133]; Neuroma[131]
Tibial neuropathy - TTS or Proximal tibial neuropathy	Increased CSA at or distal to the tarsal tunnel (cf. median nerve) can be seen in the[134]: Tibial nerve, Medial plantar and Lateral plantar nerves; Using the following cut-off values for the tibial nerve within the tarsal tunnel[134]:	Intraneural and fascicular hypoechogenicity[135]	NA	Identification of underlying aetiology of TTS; Ultrasound identifies 60-80%[136,137]; Preoperative US assessment identifies[136,138-140]: Ganglia (7-58%), Talocalcaneal coalition +/- ganglia, Varicose veins (18- 6%), Accessory soleus and flexor digitorum muscles (6%)

	> 19 mm² - Sensitivity 61%, Specificity 88%			Multiple sites of compression frequently seen in the tarsal tunnel and more distal or proximal[137]
	Within tunnel-to-proximal tunnel CSA ratio > 1[134]			Identification of underlying aetiology in proximal tibial neuropathies[141-143]: Baker's cysts, intraneural ganglion cysts, deep vein thrombosis, popliteal artery aneurysms, soleal sling
	Measured within the tarsal tunnel, proximal and inferior to the medial malleolus, and 4 cm proximal at the upper border of the medial malleolus			
	Sensitivity 74%, Specificity 100%			
	Best to compare CSA to contralateral side			
Neurogenic thoracic outlet syndrome	Enlarged CSA of lower trunk of the brachial plexus[144]	Hypoechogenicity of the lower trunk of brachial plexus[144]	NA	Alternate aetiologies[144-147]:
	Affected - 32.5 mm² (range: 20-50 mm²)	Loss of fascicular structure[144]		Cervical rib
	Controls – 16.7 mm² (range: 9-23 mm²)	Hyperechoic fibromuscular band (wedge shaped) adjacent to the middle scalene muscle – indenting the lower trunk of the brachial plexus (sickle shaped)[144]		Anomalous muscular insertion (scalene muscle between subclavian artery and brachial plexus)
		"Wedge-sickle" sign		Brachial plexus branching variants
		Sensitivity 95%, PPV 82.6%		Subclavian arterial occlusion with dynamic movement
				Sonographic Tinel's sign[144]
				Sensitivity of 55% (95% CI: 31.53%–76.94%)
				PPV of 100% (95% CI: 71.51%–100.00%)

CTS: Carpal tunnel syndrome; CSA: Cross-sectional area; ULN: Upper limit of normal; WFR: Wrist to forearm ratio; US: Ultrasound; EDX: Electrodiagnostics; PPV: Positive predictive value; UNE: Ulnar neuropathy at the elbow; PIN: Posterior interosseous syndrome; NA: Not available; LFCN: Lateral femoral cutaneous neuropathy; MP: Meralgia paraesthetica; TTS: Tarsal tunnel syndrome; LFC: Lateral femoral cutaneous; CI: Confidence interval.

reports, which evaluated median nerves to the mid forearm, did not find any significant differences between median nerve CSA and fascicle diameters in CMTX cohorts and healthy controls[27,150]. However, more recent studies, which evaluated both proximal and distal sites in the upper and lower limbs, identified consistent symmetrical enlargement in proximal nerve segments and lower limb nerves[155,159]. This finding was more pronounced in men, who are typically more significantly affected[159].

CMT2: CMT2 is a heterogenous group, with axonal neurophysiology, comprising of both autosomal dominant and recessive mutations in over 52 genes[157]. Axonal neuropathies are typically characterised by NMUS as having reduced or normal nerve dimensions, thought secondary to progressive axonal drop out[15]. However, in CMT2 variability has been seen in CSA findings with some studies identifying upper and lower limb CSAs commensurate with normal controls[155,159], and others finding slightly increased median nerve CSA compared to normal individuals[27,150]. This variability may be due to the differing pathological processes occurring in the diverse genetic subtypes of CMT2 with some, but not all, displaying endoneurial swelling, hyperplasia of Schwann cells or pseudo-onion blub formation on pathological specimens[160].

In summary, NMUS can be used to differentiate axonal and demyelinating forms of CMT, and further patterns are being identified to discriminate specific genetic subtypes. Recently a scoring system has been proposed to facilitate this distinction

using differing combinations of distal, proximal and sural nerve CSAs as well as entrapment ratios to stratify CMT1A, CMT1B, CMTX and CMT2[159]. Future studies in large cohorts will be required to assess the utility of this score in differentiating between genetic subtypes of CMT, and between CMT and acquired neuropathies. In the future NMUS will be increasingly useful as a non-invasive test in children with suspected CMT and can also be used, with EDX, to guide targeted gene testing. In addition, NMUS could be used as a disease monitoring tool for clinical trials, in particular in the setting of absent motor or sensory potentials or severe muscle atrophy. A study of quantitative muscle US demonstrated that the thickness and echogenicity of the first dorsal interosseous and tibialis anterior correlated with disease severity, and this too could be used as a surrogate marker of disease progression in clinical trials[161].

HNPP: HNPP, previously known as tomaculous neuropathy due to the focal thickening of myelin (tomacula) seen on nerve biopsy, is characterised by recurrent, painless mononeuropathies at sites of entrapment[157]. Multiple, focal enlargements of nerves, without increased vascularity, have consistently been identified in HNPP at typical sites of entrapment[151,155,159,162-165]. However, some studies have also identified enlarged CSA at sites of non-compression, even in clinically unaffected nerves[164]. Padua *et al*[155] identified ulnar nerve CSA enlargement in all patients with HNPP in their cohort and suggested more frequent involvement of the ulnar nerve, than the median nerve, in HNPP.

In most cases the CSA does not correlate with electrophysiologic or clinical characteristics[162]. Specifically, Gianneschi *et al*[165] found no sonographic changes in the distal nerves despite increased distal motor latencies. However, in one case report digital nerve enlargement has been reported[166], suggesting that further US evaluation of the distal nerves may be worthwhile in future studies. HNPP may be distinguished from forms of CMT through the use of entrapment ratios, with a CSA of the compressed nerve segment to non-compressed segment ratio greater than 1.4[150,151,159] and normal CSA at non-compressed areas. This is particularly evident as CMT1A and MPZ-associated CMTs do not typically display significant nerve enlargement at entrapment sites[149].

ATTRv amyloidosis: ATTRv amyloidosis, caused by over 130 point mutations in the transthyretin (TTR) gene, is an inherited autosomal dominant condition characterised by cardiomyopathy, frequent CTS, and an axonal, sensorimotor, peripheral neuropathy involving the large, small and autonomic nerve fibres. TTR is produced predominantly in the liver and is excreted as a tetramer, with roles in transport of Vitamin A and Thyroxine. Point mutations destabilise the molecular structure of TTR facilitating dissociation into monomers and amyloid fibril formation. Pathologically the amyloid fibrils accumulate in the extracellular space causing damage to involved tissues. Sural nerve biopsy specimens confirm intraneural amyloid accumulation with associated axonal loss.

As such, and in contrast to other typical axonal neuropathies, NMUS is expected to identify thickened peripheral nerves. Initial studies of MRI Neurography in ATTRv amyloidosis have confirmed this hypothesis (Figure 2F)[167,168]. An initial study of NMUS, by Granata *et al*[169], of 7 patients with ATTRv identified multifocal enlargements of both distal and proximal upper limb nerves, with a normal NMUS in 1 patient with only mild sensory polyneuropathy. Interestingly the number of nerves involved on NMUS correlated with disease severity[169]. Further studies in larger cohorts have confirmed significantly larger CSA in both the upper and lower limbs, with most dramatic enlargements at entrapment sites and in proximal nerves[170]. Asymptomatic ATTRv carriers were compared with symptomatic ATTRv patients and healthy controls and found to have intermediate CSA, particularly in proximal nerve segments[170]. Median CSA enlargement was found to correlate with reducing compound muscle action potential amplitudes[170]. Ongoing research is required to confirm these initial findings; however, it is expected that NMUS could be a useful tool for monitoring progression and response to treatments in ATTRv amyloidosis.

Sensory neuronopathies

Cerebellar ataxia, neuropathy, CANVAS: CANVAS is an increasingly recognised cause of late onset ataxia with cardinal features of cerebellar ataxia, bilateral vestibulopathy and a sensory neuronopathy[171]. An intronic repeat expansion (AAGGG) of the replication factor C subunit 1 gene has recently been described with a carrier frequency of 0.7% in Europeans[171]. Pelosi *et al*[172] have evaluated the median, ulnar, tibial and sural CSAs in CANVAS patients finding significantly smaller CSAs compared with both normal controls and axonal, acquired neuropathy controls. When compared to the healthy control population, the reduction in CSA in individuals with

CANVAS was sufficient to detect all but one case (93%, 13/14)[172]. Thus, NMUS has been proposed as a potential diagnostic tool for the sensory neuronopathy seen in CANVAS[172]. A follow-up study has identified that the reduction in CSA, with a cut-off of < 5 mm^2 for the median and ulnar nerves at the mid-forearm and mid-humerus, has high diagnostic accuracy to discriminate CANVAS patients from healthy controls (AUC ROC 0.97-0.99)[173].

Pathological studies in CANVAS have demonstrated marked atrophy of dorsal root ganglia with corresponding near-complete neuronal loss and posterior column atrophy[174]. Furthermore, sural nerve biopsy specimens in CANVAS display severe axonal loss without Schwann cell proliferation or active Wallerian degeneration[175]. Suggesting that the reduction in the CSA in CANVAS is due to profound axon depletion without marked connective tissue replacement, as can be seen in some types of CMT2.

SCA: Spinocerebellar ataxia type 2 (SCA2), caused by an autosomal dominant, CAG triplet expansion in the Ataxin 2 gene, is a cerebellar plus syndrome characterised by cerebellar ataxia, sensory and/or motor peripheral deficit, pyramidal signs, extrapyramidal features and sleep disorders. Peripheral nerve involvement is thought to be present in 92% of individuals with SCA2[176], with reduced sensory action potentials seen in asymptomatic carriers up to 8 years before manifestation of cerebellar signs[177]. However, it is uncertain if the sensory and motor involvement is due to a neuropathy or neuronopathy. Thus, the NMUS findings seen in CANVAS has led to further interest in US and pathological characteristics of the sensory deficits seen in SCA2. In 7 selected patients with genetically confirmed SCA2 and a sensory, axonal, non-length dependent neuropathy, Leadbeatter *et al*[173] identified that SCA2 patients had similarly reduced nerve CSAs to the CANVAS cohort. Specifically, all patients met the CANVAS diagnostic cut-off criteria (< 5 mm^2) for the median forearm site and all but one (86%) met criteria for the median-mid humerus and ulnar sites[173]. In a larger study 74% (20/27) of patients with SCA2 had reduced upper limb CSAs[178]. Of the remaining 7, 2 had increased and 5 normal range upper limb CSA[178]. Interestingly none of the patients with small nerves had a definite length-dependent sensory neuropathy, and conversely none of the patients with a definite non-length dependent sensory neuropathy had normal or enlarged nerves[178]. Taken together, this suggests that in SCA2 there may be multiple pathological contributors to the sensory deficits, including both a dorsal root ganglionopathy and peripheral neuropathy. Furthermore, these findings demonstrate that the diffuse reduction in CSA reflects a dorsal root ganglionopathy causing a sensory neuronopathy, rather than being specific for a particular disease process.

FRDA: FRDA, caused by a GAA trinucleotide repeat expansion in the frataxin gene, is the most common autosomal recessive ataxia syndrome. FRDA typically presents with cerebellar ataxia, cardiomyopathy, diabetes and skeletal malformations. Sensory deficits are common, and similar to SCA2, this may be explained by either a dorsal root ganglionopathy or peripheral neuropathy. Pathological studies have demonstrated both structurally abnormal and atrophied dorsal root ganglia and posterior columns, as well as hypomyelination on sural nerve biopsy specimens[179,180].

Interestingly Mulroy *et al*[181] found that in FRDA almost all tested upper limb nerves had significantly larger CSAs and common fascicular enlargement. The CSA was typically 2 standard deviations greater than the CSA of normal controls[181]. However, there was no difference in the lower limb CSA in the FRDA patients compared to controls. The enlargement of CSA in the upper limbs may be due to perineural connective tissue infiltration, inflammation and dysmyelination with impaired Schwann cell interactions[182]. Whereas the normal CSA seen in lower limbs may reflect the more pronounced caudal ganglionopathy as well as peripheral nerve processes[181]. Further NMUS in FRDA, in particular at earlier disease stages, will be useful to delineate the pathogenesis of these findings.

Immune-mediated peripheral nerve disorders

CIDP: Clinical manifestations of typical CIDP are symmetrical, proximal and distal weakness, sensory disturbance and hypo- or areflexia. Pathological nerve specimens characteristically display focal and segmental demyelination, with subsequent remyelination, leading to the formation of onion bulbs, accompanied by endoneurial inflammation and oedema[183]. As such NMUS was hypothesised to show multifocal enlargements of CSA in proximal and distal segments with hypervascularity. While the majority of patients do indeed have enlargement in CSA on NMUS, in both proximal and distal segments and at non-entrapment sites[15,184-189], there is marked variability with some patients having normal or mildly enlarged nerves (Figures 2B, 2D and 3C)[190]. Padua *et al*[190] describe three different classes of sonographic findings,

which correlate with disease duration. Specifically, Class 1 nerves have increased CSA with hypoechoic fascicles, Class 2 increased CSA with mixed hypo- and hyper-echoic fascicles, and Class 3 normal CSA with hypoechoic fascicles. The latter class was associated with more prolonged disease durations. Hence it is suggested that NMUS findings may the parallel disease stages and reflect the underlying pathophysiology in CIDP. This hypothesis is further supported by studies which have found improvement in nerve calibre in patients who reach clinical and electrophysiological remission after treatment for CIDP[185].

Hypervascularity of nerves can be seen in CIDP and correlates both with the number of nerves with enlarged CSA and cerebrospinal fluid (CSF) protein levels[38]. Similarly the calibre of cervical nerve roots, which are commonly enlarged in CIDP, correlates with CSF protein levels and disease duration[186,191]. Taken together, both the vascularity and number of enlarged nerves may be used in the future as objective measures of disease activity.

CSA negatively correlates, in some studies, with nerve conduction velocity[15,187,189]; however, this has not been ubiquitously identified[184,192]. This likely, in part, reflects the heterogeneity of US and electrodiagnostic protocols, as well as disease duration, treatment exposure and response. Further studies with more homogenous inclusion criteria will be required to delineate these findings.

Differentiation of hereditary and acquired demyelinating neuropathies and between acquired demyelinating neuropathies has recently been a focus of investigation. The major distinguishing feature between NMUS in CMT and CIDP is non-homogeneity of CSA enlargement[152]. As such the use of intranerve and internerve CSA variability has been proposed, and is significantly larger in CIDP than CMT[158,193,194]. A multitude of additional US rating scores have been proposed to aid the differentiation of acquired and hereditary demyelinating neuropathies including the ultrasound pattern sum score (UPSS), homogeneity score, regional nerve enlargement index, Bochum US score, and nerve abnormality index[155,188,195,196]. The usefulness of these scores will require further investigation in large cohorts in order to rationalise and standardise use internationally.

Guillain-Barre syndrome: Similar to CIDP, NMUS in Guillain-Barre syndrome (GBS) typically identifies proximal more so than distal enlargement of nerve calibre. Although the degree of enlargement of CSA is less than both CMT1A and CIDP, and is patchier[15,197]. Again marked variability in CSA findings are seen with the percentage of patients with enlarged CSA ranging from 0%-67%[15,152,195,197]. This likely reflects heterogeneity in the clinical populations included in studies comprising of both axonal and demyelinating forms, and at differing time points of disease. Nerve enlargement can be identified as early as 1 d after onset and can be seen prior to neurophysiological changes[15,198]. Persistent nerve enlargement has been reported up to 15 years, often not correlated with disability, although other reports suggest normalisation of NMUS findings with clinical remission[15,199-201]. Studies evaluating NMUS across the temporal evolution of GBS are required to solidify the spectrum of normal findings in GBS. If early nerve root enlargement is consistently confirmed, NMUS could allow early diagnosis of GBS to be made, and hence limit morbidity.

A few studies have compared axonal and demyelinating forms of GBS. Razali *et al*[201] found no significant differences in CSA between acute demyelinating polyneuropathy (AIDP) and acute motor (and sensory) axonal neuropathy (AMAN/AMSAN). In contrast, Mori *et al*[202] identified different patterns of disease with AIDP having enlarged cervical roots and proximal nerve segments, and AMAN enlarged distal segments. Enlarged vagus nerve CSA has been identified in patients with autonomic dysfunction in both demyelinating and axonal forms of GBS[188,198].

The UPSS has been proposed to differentiate CIDP, GBS and axonal neuropathies. In the UPSS enlarged cervical and vagal CSA, but minimal-moderate enlargements in the upper and lower extremity nerves is thought suggestive of GBS, compared with more marked increases in limb nerve CSA and total scores being reflective of CIDP[188]. An alternate score, the Bochum ultrasound score, evaluates the CSA of the ulnar nerve at Guyon's canal and in the arm, the radial nerve at the spiral groove and the sural nerve at the calf, giving each one point if enlarged compared to normal controls[195]. A cut off score of greater than 2 had a sensitivity of 90% and specificity in 90.4% in distinguishing CIDP from GBS. Further studies are required to assess the utility of scoring systems in distinguishing these inflammatory neuropathies.

Multifocal acquired demyelinating sensory and motor neuropathy: In Multifocal acquired demyelinating sensory and motor neuropathy (MADSAM), a variant of CIDP characterised by asymmetric and patchy sensorimotor impairments and neurophysiology, NMUS typically demonstrates multifocal CSA enlargement at sites of current or resolved conduction block[203-205]. In one case these nerve swellings appear

to be treatment responsive, with early and complete clinical and electrophysiological remission after intravenous immunoglobulin[206]. Similar to CIDP, nerves in MADSAM are hypoechogenic with enlarged hypoechogenic nerve fascicles at sites of maximal CSA (Figure 2C)[203], and vagus nerve enlargement can be seen[207]. However, nerve enlargements in MADSAM are more asymmetrical, heterogenous, and segmental than commonly seen in CIDP. Taken together these findings suggest that US parameters could be used in the future as a biomarker of ongoing disease activity, treatment response and prognosis in MADSAM.

MMN: MMN is a slowly progressive, immune-mediated, upper limb predominant motor neuropathy with conduction block, at sites of non-compression, typically seen on neurophysiology. MMN can be difficult to diagnose often requiring extensive proximal neurophysiology to identify demyelination and conduction block to distinguish it from mimics including amyotrophic lateral sclerosis (ALS), progressive muscular atrophy and pure-motor CIDP. NMUS has been recently evaluated as a tool to differentiate these entities. Studies have predominantly focused on CSA, identifying in the vast majority of patients with MMN moderate, segmental nerve enlargement primarily in proximal nerves, and at sites with and without neurophysiological evidence of conduction block[29,152,208-210]. The presence of multifocal increases in nerve calibre distinguishes MMN from ALS and normal controls, with sensitivities of 87%-100% and specificities of 92%-100%[208,209,211]. A recent comparison of MR Neurography and US, demonstrated that US was better able to distinguish inflammatory neuropathies, including CIDP and MMN, from segmental SMA (sSMA) by identifying proximal CSA enlargements[212]. As such, US has been proposed as a tool to aide treatment decision making[213]. The NMUS of CIDP and MMN are more similar, both showing multifocal nerve enlargements; however, studies attempting to differentiate these entities has identified greater increases in CSA in CIDP and greater intra-nerve, inter-nerve and side-to-side intra-nerve variability in MMN[193,214,215].

Attempts to prognosticate with NMUS has led to inconsistent results[209,210,215]; however, some studies suggest that CSA reduces with more severe disease, as a correlate to axonal loss, signifying that serial NMUS in individuals with MMN could possibly play a role in prognostication and guide treatment escalation[29,214]. Further evaluations in more homogenous MMN cohorts, with serial measurements prior to, and after treatment will be required to further delineate the role of NMUS in diagnostic and treatment algorithms.

Brachial neuritis: Brachial neuritis, also known as neuralgic amyotrophy or Parsonage-Turner Syndrome, is an idiopathic inflammatory condition affecting the motor and sensory nerves of the brachial plexus heralded by severe neuropathic pain. Precise localisation of a plexus lesion is often difficult with EDX alone, and NMUS has the potential to more precisely localise pathology within the plexus and identify possible compressive lesions. Initial NMUS studies suggest median, isolated anterior interosseous or posterior interosseous enlargement on the affected side compared to both healthy controls and the individuals unaffected side[216,217]. A detailed study by Aranyi *et al*[218] has identified more varied pathologies including focal or diffuse nerve and fascicle enlargement in 57%, incomplete nerve constriction in 36%, complete nerve constriction with hour-glass torsions in 50% and fascicular entwinement in 28%.The torsions seen on NMUS were confirmed surgically, and were present in the radial nerve in 85% of cases. It is hypothesised that in brachial neuritis the nerve first enlarges, with ongoing inflammation adhesions and fixation of the fascicles cause it to constrict, and then with rotational movements of the limb nerve torsion develops. It is suggested that fascicle entwinement is most likely analogous to nerve torsion. The presence of constriction, torsion or fascicular entwinement correlates with limited functional improvement with conservative measures alone, and may even require surgical intervention[219]. This suggests an important and management altering role for NMUS, or alternate imaging, in the acute evaluation of individuals with brachial neuritis.

Vasculitic neuropathy: In both systemic and isolated peripheral nerve vasculitis the typical neuromuscular presentation is of a mononeuritis multiplex due to inflammation of epineurial vessels causing an ischaemic insult to affected nerves. On NMUS focal, asymmetrical enlargement of nerve CSA can be seen in 51-71% of clinically and neurophysiologically affected nerves, with nerve hypoechogenicity and enlargement of single fascicles[39,220-223]. Üçeyler *et al*[224] identified preferential involvement of the sural and superficial peroneal nerves. Multifocal nerve enlargement proximal to compression site was 94% sensitive and 88% specific for vasculitic neuropathy in one cohort[222]. Hypervascularity has also been seen in a smaller proportion of patients with vasculitic neuropathy[222]. Goedee *et al*[222] proposed

that in an axonal neuropathy, multifocal enlargement of nerves proximal to entrapment sites, with sparing of the brachial plexus, may be characteristic of vasculitic neuropathies. Limited published data exists for the NMUS response to treatment; however, in one case study treatment resulted in reduced calibre of single nerve fascicles and the overall nerve, although no changes were seen in nerve echogenicity[220].

In summary, NMUS may facilitate early diagnosis, and hence earlier treatment commencement in vasculitic neuropathies, and could be used to identify optimal sites for nerve biopsy. Further studies are required to evaluate the responsiveness of NMUS to treatment and to solidify the pattern of nerve involvement in vasculitic neuropathy, in particular in comparison to other axonal neuropathies with enlarged nerve CSA, such as hereditary ATTRv amyloidosis.

Anti-myelin-associated glycoprotein neuropathy: Neuropathy associated with anti-myelin-associated glycoprotein (MAG) antibodies is typically described as a distal acquired demyelinating symmetric phenotype, with characteristic prolongation of distal motor latencies on neurophysiology. One study has evaluated the NMUS properties of anti-MAG neuropathies showing segmental, but not distal, increased nerve CSA, with greater intranerve than internerve variability[225]. The US phenotype was intermediate between axonal paraproteinaemic neuropathy controls and IgM paraprotein-associated CIDP. More recently Garg *et al*[226] demonstrated no distal nerve enlargement, but significant proximal nerve enlargement compared to healthy controls, specifically of the C6 nerve root and upper trunk of the brachial plexus. To date enlarged distal nerve calibre has not been identified, which is at odds with the characteristic neurophysiological findings. This suggests that the proximal nerve segments may be more involved than previously thought and possibly underestimated by neurophysiological tests due to the prominent distal nerve slowing.

Polyneuropathy, organomegaly, endocrinopathy, M-protein, skin changes syndrome: The neuropathy of polyneuropathy, organomegaly, endocrinopathy, M-protein, skin changes (POEMS) syndrome is characteristically of mixed axonal and demyelinating neurophysiology, with motor predominant distal weakness affecting dorsiflexion more so than plantarflexion[227]. Early in the disease course, the neuropathy of POEMS can mimic CIDP, with more predominant demyelinating features. In contrast to CIDP, US of distal and proximal limb nerves identified enlargement of CSA at sites of entrapment in POEMS, but not at other sites along the nerves[228]. It must be noted that in all studied patients there were clinical and neurophysiological signs of secondary axonal degeneration at the time of NMUS. Concordant with this, a large neve biopsy series recently demonstrated higher axonal degeneration, minimal endoneurial inflammation and higher numbers of epineurial vessels in POEMS than CIDP; however, the timing of biopsy after disease onset is not clear[229]. While the pathophysiology of neuropathy is incompletely understood, it is thought associated with increased neovascularisation due to elevated circulating vascular endothelial growth factor, and impaired blood nerve barrier causing increased neural oedema[229]. Thus, it would be postulated that in early disease increased CSA and vascularity may be appreciated. Further studies in the early diagnostic setting will be required to further evaluate the NMUS features of POEMS syndrome and may assist in clarifying the underlying pathophysiology.

Neurolymphomatosis: Nerve infiltration by lymphoma, or neurolymphomatosis, typically causes focal mononeuropathies or plexopathies, and can be the presenting symptom or site of recurrence of systemic lymphomas. Case reports and series have demonstrated enlarged nerve calibre of affected nerve segments, hypoechoic echotexture, with enlarged fascicles and hypervascularity suggestive of infiltration and neovascularisation[37,230]. Further studies are required; however, in the future NMUS may play a role in diagnosis, surveillance and optimisation of nerve biopsy in neurolymphomatosis.

Motor neuron diseases
Diseases of motor neuron degeneration include ALS, and SMA, which differ in age of onset and aetiology. ALS is typified on NMUS by reduced distal and proximal nerve calibre (Figure 3A)[231-235]. Analogous to what has been demonstrated in the pure sensory neuronopathies, this is hypothesised to be due to motor axon loss due to anterior horn cell degeneration. In addition a recent study identified increased wrist-upper arm ratios in ALS compared with controls, and a combination of reduced CSA and distal-proximal ratios had diagnostic value in distinguishing ALS from mimics[235].

In contrast, while not extensively studied to date, NMUS in sSMA has

demonstrated reductions in CSA in the proximal nerve segments and nerve roots only, when compared to the CIDP and MMN[212]. A feature which could, if confirmed in additional studies, be used to differentiate adult onset SMA from ALS. Ultra-high frequency US has been used in a small cohort of SMA types I, II and III patients, and controls to evaluate nerve area, fascicle numbers and densities[26]. Interestingly differences were only observed in fascicle number between the SMA I patient and controls, suggesting that alterations in the number and density of fascicles could be used to prognosticate in SMA[26]. However, further studies in larger cohorts are required to confirm this finding.

Schreiber *et al*[232] assessed the CSA of the median and ulnar nerves at the wrist and forearm in ALS subtypes, finding reduced ulnar, but not median CSA, in all ALS subtypes except for primary lateral sclerosis (PLS). This suggests the possible value CSA measurements as an indicator of lower motor neuron dysfunction in ALS, which has prognostic implications in particular in distinguishing upper motor neuron dominant ALS from PLS. As mentioned previously NMUS may also play a role in distinguishing potentially treatable lower motor neuron diseases, such as MMN, from non-treatable, with significant prognostic implications.

Beyond the scope of this review, but relevant in motor neuron disorders, is the use of muscle US, which has been more extensively investigated in ALS and SMA. In brief, muscle US identifies patchy increased echogenicity and atrophy in these conditions, and in some studies correlates with strength[231,233,236-238]. US is a more sensitive tool than EMG for identifying fasciculations, in all muscles; however, particularly in the tongue[238-242]. Hence muscle US plays an important role in ALS diagnostics as a biomarker of lower motor neurone involvement, and may allow earlier diagnosis[238,239]. In addition identification of widespread fasciculations, using a score of 9 muscles, can assist to distinguish ALS and mimics with a 92% sensitivity and 100% specificity[241].

Muscle US also allows the evaluation of more difficult to assess muscles, including the tongue and diaphragm, where EMG is more difficult or has potential side effects[242]. This is particularly important in ALS, where dysfunction of these muscles has prognostic implications. For example the alteration in diaphragm thickness during inspiration and expiration correlates with respiratory function measures in ALS including forced vital capacity, maximum voluntary ventilation and sniff nasal inspiratory pressure, as well as diaphragm compound muscle action potential[243]. A recent longitudinal study has demonstrated that serial US measurements can more accurately predict the need to initiate non-invasive ventilation when compared with respiratory function tests[244]. In addition, dynamic assessment of the bulbar muscles, by evaluating the maximum thickness of the mylohyoid-geniohyoid-muscle-complex during swallowing and at rest, can be performed and correlates with the severity of upper motor neuron involvement in ALS[245]. As such, NMUS will likely become an increasingly utilised non-invasive longitudinal biomarker in ALS, with use in both the diagnostic and prognostic settings.

Axonal neuropathies

To date NMUS has limited utility in axonal neuropathies. It was anticipated that, similar to ALS, NMUS findings in axonal neuropathies would identify reduced CSA of nerves. Instead normal or mildly enlarged nerve calibres are typically seen[15,39]. In all subtypes of diabetic peripheral neuropathy (DPN), for example, there is mild enlargement of nerve CSA, fascicular enlargement and loss of the normal fascicular architecture, with particular enlargements seen at sites of compression[246-251]. Nerve enlargement can also be seen in diabetics prior to the development of DPN[251]. In some studies the CSA enlargement, thought due to increased water content, has negatively correlated with both compound muscle action potential amplitudes and motor nerve conduction velocities[247,250]. Increased vascularity has also been demonstrated in diabetic nerves, and corelate with nerve calibre, sensory symptoms and the severity of neuropathy[49]. Recently shear wave elastography has been assessed in the tibial nerves of healthy controls, patients with diabetes and diabetic neuropathies, finding a continuum of increasing stiffness[252]. A cut-off value of 51 kPa was found to be highly specific and sensitive for the diagnosis of DPN[252].

Similarly, in chemotherapy associated neuropathies focal enlargements at sites of nerve entrapment is observed[253,254]. This can be seen in asymptomatic individuals, suggesting the chemotherapeutics may increase the susceptibility of nerves to additional damage[253]. While these changes are subtle, these findings suggest that NMUS may play a role in monitoring for increasing susceptibility to nerve damage, and hence may guide treatment alterations.

In axonal neuropathy associated with monoclonal gammopathy of uncertain significance and multiple myeloma typically no nerve enlargement is found[255,256]. However, in two cases where nerve enlargement was identified in this axonal cohort,

management was altered to include immunotherapy with a beneficial outcome[255], suggesting that nerve enlargement may also facilitate therapeutic decision making in these paraproteinaemic axonal neuropathies. However, in general the role of NMUS in the diagnosis, management or prognostication of multiple axonal neuropathies, including due to infections, inflammatory, toxic or metabolic insults, is not yet known. Future studies are required delineate the role of NMUS in these contexts.

THE CURRENT AND FUTURE ROLE OF NMUS IN THE MANAGEMENT OF PERIPHERAL NERVE DISORDERS

NMUS is now commonly used to guide procedures such as peripheral nerve blocks, steroid injections for entrapment neuropathies and botulinum toxin injections for spasticity and dystonia. There is growing interest in its use for guidance of nerve conduction and EMG. The use of NMUS to determine the optimal site for nerve and muscle biopsy and lumbar puncture is currently gaining further traction. In addition NMUS has more recently been used in the intensive care setting to identify post-operative diaphragmatic palsies, and hence is a useful tool to predict and prevent respiratory decline after extubation[257,258].

NMUS is also increasingly being used to guide surgery. NMUS has been used to identify normal neural tissue pre- and intra-operatively in the resection of nerve sheath tumours and after trauma, hence allowing the identification and informed consent for the risk of iatrogenic nerve damage, and guiding optimal micro- or macro-surgical approaches[20,259,260]. In addition, pre-operative identification of nerve position and anatomical variants with NMUS can prevent iatrogenic transection, as can occur in the sural nerve, for example, during small saphenous vein stripping, and can guide further management including transposition and neurolysis[261]. Furthermore, NMUS frequently identifies true entrapment of the interrogated nerve, in particular in the ulnar nerve at the elbow or peroneal neuropathy at the fibular head, and hence can stratify patients who can be managed conservatively versus those who require surgical decompression[113,114,128].

New techniques are also being developed using US technology for the management of peripheral nerve disorders. US guided minimally invasive carpal tunnel release is increasingly being used, in both surgical and primary care settings, for rapid, carpal tunnel decompression with good clinical outcomes[262-265]. Specifically, these techniques allow concurrent bilateral decompressions, earlier functional recovery and less post-operative morbidity with equivalent neurological outcomes to mini-open carpal tunnel release[262-264]. In addition pulsed, low-frequency US has been used for non-invasive neuromodulation in compressive neuropathy and radiculopathy reducing pain and improving quality of life in affected individuals[266]. With the greater availability of NMUS, ongoing technical advances and expanding interest in the techniques, the use of NMUS for therapeutic intervention will most likely dramatically increase over the coming years.

PRACTICAL CONSIDERATIONS

NMUS is a rapidly expanding area of clinical practice and research, with significant potential to alter diagnostic and treatment paradigms in neuromuscular medicine. However, there are barriers to mainstream uptake of the technology including substantial costs of equipment, adequate teaching experience and current gaps in knowledge and applicability. Recent developments in technology have begun to reduce the financial strain associated with US unit purchase, with more economical laptop-based units and US integrated into EMG machines providing adequate resolution for the evaluation of nerves in most regions of interest. Once equipped, NMUS in mononeuropathy cohorts is reported to improve quality of life outcomes, with only modest outlays on cost-effectiveness analyses[267,268]. While these initial studies suggest a positive benefit-outlay ratio, the overall cost-effectiveness of NMUS for diagnostics, monitoring and prognostication in neuromuscular diseases is not yet known. However, it seems reasonable that the initial equipment outlays are warranted in the context of improved patient care[269].

The availability of training in NMUS is another potential barrier for the widespread uptake of peripheral nerve US. At present most training is undertaken though a practical traineeship supervised by a skilled mentor and supplemented with intermittent courses. However, the availability of apprenticeships, in particular in some geographical areas, is limited, and there is no standardised curriculum or teaching structure. The American Association of Neuromuscular and

Electrodiagnostic Medicine has developed guidelines to direct training in both clinical and technological aspects of NMUS[270]. However, standardisation, assessment and accreditation processes should also be developed to provide certification for both supervisors and training sites.

Similarly, standardisation of processes and methodology for investigation of polyneuropathies would be worthwhile to aid research, allowing more robust comparisons to be made between sites. Furthermore, there has been a vast proliferation of scoring systems made in parallel, for different neuromuscular indications, which can lead to confusion and ultimately requires further rationalisation. In the future meta-analyses integrating geographically separate, but comparable, data and consensus scoring systems should be advocated for in order to improve our collective understanding of NMUS in different disease processes and in different ethnic groups.

Finally, Medicolegal issues may arise in NMUS if pathologies are missed, incorrectly reported or over-reported leading to morbidity or mortality. This is particularly the case for non-neural tissues. As such, it is recommended that NMUS reports stipulate that evaluation was limited to neuromuscular structures, and that any atypical features in other tissues identified should be further assessed by experienced radiologists with additional imaging modalities[269].

CONCLUSION

NMUS is becoming an integral component of the diagnostic and management algorithm in neuromuscular medicine. As a non-invasive and accessible tool, it provides excellent resolution and dynamic assessment of neural structures. Hence adding much needed information about structure and function to clinical examination and EDX. Multiple studies have shown a role for NMUS in the diagnosis, monitoring and management of peripheral nerve disorders, and the applications of NMUS continues to expand. Recognition of the patterns of sonographic changes in differing aetiologies of peripheral neuropathy may assist to streamline diagnostic processes, improving time to diagnosis, accrued disability and health-care expenditure. Further exploration of novel techniques for the evaluation of peripheral nerves, may provide additional insights into the underlying pathophysiology of peripheral nerve diseases, and targets for therapeutic modification. Increasing standardisation of existing techniques and the creation of consensus scoring systems will allow improved reproducibility of findings, and greater applicability of results to clinical reasoning. Improved understanding of current and novel NMUS techniques will provide increasing insights into the pathophysiology of nerve diseases, and comparisons with clinical, electrodiagnostic and histopathological characteristics is necessary to clarify the roles of NMUS in the future.

REFERENCES

1   **Fornage BD**. Peripheral nerves of the extremities: imaging with US. *Radiology* 1988; **167**: 179-182 [PMID: 3279453 DOI: 10.1148/radiology.167.1.3279453]

2   **Solbiati L**, De Pra L, Ierace T, Bellotti E, Derchi LE. High-resolution sonography of the recurrent laryngeal nerve: anatomic and pathologic considerations. *AJR Am J Roentgenol* 1985; **145**: 989-993 [PMID: 3901711 DOI: 10.2214/ajr.145.5.989]

3   **Gallardo E**, Noto Y, Simon NG. Ultrasound in the diagnosis of peripheral neuropathy: structure meets function in the neuromuscular clinic. *J Neurol Neurosurg Psychiatry* 2015; **86**: 1066-1074 [PMID: 25653385 DOI: 10.1136/jnnp-2014-309599]

4   **Buchberger W**, Schön G, Strasser K, Jungwirth W. High-resolution ultrasonography of the carpal tunnel. *J Ultrasound Med* 1991; **10**: 531-537 [PMID: 1942218 DOI: 10.7863/jum.1991.10.10.531]

5   **Simon NG**, Narvid J, Cage T, Banerjee S, Ralph JW, Engstrom JW, Kliot M, Chin C. Visualizing axon regeneration after peripheral nerve injury with magnetic resonance tractography. *Neurology* 2014; **83**: 1382-1384 [PMID: 25186862 DOI: 10.1212/WNL.0000000000000861]

6   **Eppenberger P**, Andreisek G, Chhabra A. Magnetic resonance neurography: diffusion tensor imaging and future directions. *Neuroimaging Clin N Am* 2014; **24**: 245-256 [PMID: 24210323 DOI: 10.1016/j.nic.2013.03.031]

7   **Morrow JM**, Sinclair CD, Fischmann A, Machado PM, Reilly MM, Yousry TA, Thornton JS, Hanna MG. MRI biomarker assessment of neuromuscular disease progression: a prospective observational cohort study. *Lancet Neurol* 2016; **15**: 65-77 [PMID: 26549782 DOI: 10.1016/S1474-4422(15)00242-2]

8   **Walker F**, Cartwright M. Neuromuscular ultrasound. 1st ed. Philadelphia: Elsevier, 2012: 37-56

9   **Simon NG**, Noto YI, Zaidman CM. Skeletal muscle imaging in neuromuscular disease. *J Clin Neurosci* 2016; **33**: 1-10 [PMID: 27612670 DOI: 10.1016/j.jocn.2016.01.041]

10   **Pillen S**, Arts IM, Zwarts MJ. Muscle ultrasound in neuromuscular disorders. *Muscle Nerve* 2008; **37**: 679-693 [PMID: 18506712 DOI: 10.1002/mus.21015]

11   **Wattjes MP**, Kley RA, Fischer D. Neuromuscular imaging in inherited muscle diseases. *Eur Radiol* 2010; **20**: 2447-2460 [PMID: 20422195 DOI: 10.1007/s00330-010-1799-2]

12   **Zaidman CM**, van Alfen N. Ultrasound in the Assessment of Myopathic Disorders. *J Clin Neurophysiol* 2016; **33**: 103-111 [PMID: 27035250 DOI: 10.1097/WNP.0000000000000245]

13   **Walker FO**, Cartwright MS, Alter KE, Visser LH, Hobson-Webb LD, Padua L, Strakowski JA, Preston DC, Boon AJ, Axer H, van Alfen N, Tawfik EA, Wilder-Smith E, Yoon JS, Kim BJ, Breiner A, Bland JDP, Grimm A, Zaidman CM. Indications for neuromuscular ultrasound: Expert opinion and review of the literature. *Clin Neurophysiol* 2018; **129**: 2658-2679 [PMID: 30309740 DOI: 10.1016/j.clinph.2018.09.013]

14   **Tagliafico A**, Cadoni A, Fisci E, Bignotti B, Padua L, Martinoli C. Reliability of side-to-side ultrasound cross-sectional area measurements of lower extremity nerves in healthy subjects. *Muscle Nerve* 2012; **46**: 717-722 [PMID: 23055313 DOI: 10.1002/mus.23417]

15   **Zaidman CM**, Al-Lozi M, Pestronk A. Peripheral nerve size in normals and patients with polyneuropathy: an ultrasound study. *Muscle Nerve* 2009; **40**: 960-966 [PMID: 19697380 DOI: 10.1002/mus.21431]

16   **Cartwright MS**, Passmore LV, Yoon JS, Brown ME, Caress JB, Walker FO. Cross-sectional area reference values for nerve ultrasonography. *Muscle Nerve* 2008; **37**: 566-571 [PMID: 18351581 DOI: 10.1002/mus.21009]

17   **Won SJ**, Kim BJ, Park KS, Kim SH, Yoon JS. Measurement of cross-sectional area of cervical roots and brachial plexus trunks. *Muscle Nerve* 2012; **46**: 711-716 [PMID: 23055312 DOI: 10.1002/mus.23503]

18   **Haun DW**, Cho JC, Kettner NW. Normative cross-sectional area of the C5-C8 nerve roots using ultrasonography. *Ultrasound Med Biol* 2010; **36**: 1422-1430 [PMID: 20800169 DOI: 10.1016/j.ultrasmed-bio.2010.05.012]

19   **Ulaşli AM**, Tok F, Karaman A, Yaman F, Dikici O, Oruç S, Özçakar L. Nerve enlargement after cold exposure: a pilot study with ultrasound imaging. *Muscle Nerve* 2014; **49**: 502-505 [PMID: 23835853 DOI: 10.1002/mus.23947]

20   **Simon NG**, Cage T, Narvid J, Noss R, Chin C, Kliot M. High-resolution ultrasonography and diffusion tensor tractography map normal nerve fascicles in relation to schwannoma tissue prior to resection. *J Neurosurg* 2014; **120**: 1113-1117 [PMID: 24628610 DOI: 10.3171/2014.2.JNS131975]

21   **Tagliafico A**, Tagliafico G, Martinoli C. Nerve density: a new parameter to evaluate peripheral nerve pathology on ultrasound. Preliminary study. *Ultrasound Med Biol* 2010; **36**: 1588-1593 [PMID: 20850025 DOI: 10.1016/j.ultrasmedbio.2010.07.009]

22   **Boom J**, Visser LH. Quantitative assessment of nerve echogenicity: comparison of methods for evaluating nerve echogenicity in ulnar neuropathy at the elbow. *Clin Neurophysiol* 2012; **123**: 1446-1453 [PMID: 22217961 DOI: 10.1016/j.clinph.2011.10.050]

23   **Cartwright MS**, Baute V, Caress JB, Walker FO. Ultrahigh-frequency ultrasound of fascicles in the median nerve at the wrist. *Muscle Nerve* 2017; **56**: 819-822 [PMID: 28214293 DOI: 10.1002/mus.25617]

24   **Vitali S**, Rossi P, Aringhieri G, Bocci T, Barloscio D, Santin M, Sartucci F, Caramella D, editors. Very-high-resolution sonography of median nerve: A comparative study vs high-resolution sonography in healthy subjects. Proceedings of the European Congress of Radiology; 2018 Feb 28-Mar 4; Vienna, Austria [DOI: 10.1594/ecr2018/C-1508]

25   **Puma A**, Azulay N, Grecu N, Suply C, Panicucci E, Cambieri C, Villa L, Raffaelli C, Sacconi S. Comparison of high-frequency and ultrahigh-frequency probes in chronic inflammatory demyelinating polyneuropathy. *J Neurol* 2019; **266**: 2277-2285 [PMID: 31175432 DOI: 10.1007/s00415-019-09392-z]

26   **Regensburger AP**, Wagner AL, Hanslik G, Schüssler SC, Fahlbusch FB, Woelfle J, Jüngert J, Trollmann R, Knieling F. Ultra-high-frequency ultrasound in patients with spinal muscular atrophy: A retrospective feasibility study. *Muscle Nerve* 2020; **61**: E18-E21 [PMID: 31884704 DOI: 10.1002/mus.26796]

27   **Martinoli C**, Schenone A, Bianchi S, Mandich P, Caponetto C, Abbruzzese M, Derchi LE. Sonography of the median nerve in Charcot-Marie-Tooth disease. *AJR Am J Roentgenol* 2002; **178**: 1553-1556 [PMID: 12034637 DOI: 10.2214/ajr.178.6.1781553]

28   **Grimm A**, Winter N, Rattay TW, Härtig F, Dammeier NM, Auffenberg E, Koch M, Axer H. A look inside the nerve - Morphology of nerve fascicles in healthy controls and patients with polyneuropathy. *Clin Neurophysiol* 2017; **128**: 2521-2526 [PMID: 28958781 DOI: 10.1016/j.clinph.2017.08.022]

29   **Rattay TW**, Winter N, Décard BF, Dammeier NM, Härtig F, Ceanga M, Axer H, Grimm A. Nerve ultrasound as follow-up tool in treated multifocal motor neuropathy. *Eur J Neurol* 2017; **24**: 1125-1134 [PMID: 28681489 DOI: 10.1111/ene.13344]

30   **Joy V**, Therimadasamy AK, Chan YC, Wilder-Smith EP. Combined Doppler and B-mode sonography in carpal tunnel syndrome. *J Neurol Sci* 2011; **308**: 16-20 [PMID: 21764405 DOI: 10.1016/j.jns.2011.06.042]

31   **Vanderschueren GA**, Meys VE, Beekman R. Doppler sonography for the diagnosis of carpal tunnel syndrome: a critical review. *Muscle Nerve* 2014; **50**: 159-163 [PMID: 24633597 DOI: 10.1002/mus.24241]

32   **Akcar N**, Ozkan S, Mehmetoglu O, Calisir C, Adapinar B. Value of power Doppler and gray-scale US in the diagnosis of carpal tunnel syndrome: contribution of cross-sectional area just before the tunnel inlet as compared with the cross-sectional area at the tunnel. *Korean J Radiol* 2010; **11**: 632-639 [PMID: 21076589 DOI: 10.3348/kjr.2010.11.6.632]

33   **Dejaco C**, Stradner M, Zauner D, Seel W, Simmet NE, Klammer A, Heitzer P, Brickmann K, Gretler J, Fürst-Moazedi FC, Thonhofer R, Husic R, Hermann J, Graninger WB, Quasthoff S. Ultrasound for diagnosis of carpal tunnel syndrome: comparison of different methods to determine median nerve volume and value of power Doppler sonography. *Ann Rheum Dis* 2013; **72**: 1934-1939 [PMID: 23212030 DOI: 10.1136/annrheumdis-2012-202328]

34   **Ghasemi-Esfe AR**, Khalilzadeh O, Mazloumi M, Vaziri-Bozorg SM, Niri SG, Kahnouji H, Rahmani M. Combination of high-resolution and color Doppler ultrasound in diagnosis of carpal tunnel syndrome. *Acta Radiol* 2011; **52**: 191-197 [PMID: 21498348 DOI: 10.1258/ar.2010.100299]

35   **Jain S**, Visser LH, Praveen TL, Rao PN, Surekha T, Ellanti R, Abhishek TL, Nath I. High-resolution sonography: a new technique to detect nerve damage in leprosy. *PLoS Negl Trop Dis* 2009; **3**: e498 [PMID: 19668356 DOI: 10.1371/journal.pntd.0000498]

36   **Martinoli C**, Bianchi S, Gandolfo N, Valle M, Simonetti S, Derchi LE. US of nerve entrapments in osteofibrous tunnels of the upper and lower limbs. *Radiographics* 2000; **20** Spec No: S199-S213; discussion S213-S217 [PMID: 11046171 DOI: 10.1148/radiographics.20.suppl_1.g00oc08s199]

37   **Vijayan J**, Chan YC, Therimadasamy A, Wilder-Smith EP. Role of combined B-mode and Doppler sonography in evaluating neurolymphomatosis. *Neurology* 2015; **85**: 752-755 [PMID: 26231262 DOI: 10.1212/WNL.0000000000001880]

38   **Goedee HS**, Brekelmans GJ, Visser LH. Multifocal enlargement and increased vascularization of peripheral nerves detected by sonography in CIDP: a pilot study. *Clin Neurophysiol* 2014; **125**: 154-159 [PMID: 23880223 DOI: 10.1016/j.clinph.2013.05.025]

39   **Telleman JA**, Grimm A, Goedee S, Visser LH, Zaidman CM. Nerve ultrasound in polyneuropathies. *Muscle Nerve* 2018; **57**: 716-728 [PMID: 29205398 DOI: 10.1002/mus.26029]

40   **Ng ES**, Ng KW, Wilder-Smith EP. Provocation tests in doppler ultrasonography for carpal tunnel syndrome. *Muscle Nerve* 2013; **47**: 116-117 [PMID: 23180630 DOI: 10.1002/mus.23637]

41   **Borire AA**, Visser LH, Padua L, Colebatch JG, Huynh W, Simon NG, Kiernan MC, Krishnan AV. Utility of maximum perfusion intensity as an ultrasonographic marker of intraneural blood flow. *Muscle Nerve* 2017; **55**: 77-83 [PMID: 27226421 DOI: 10.1002/mus.25200]

42   **Volz KR**, Evans KD, Kanner CD, Dickerson JA. Detection of Intraneural Median Nerve Microvascularity Using Contrast-Enhanced Sonography: A Pilot Study. *J Ultrasound Med* 2016; **35**: 1309-1316 [PMID: 27151909 DOI: 10.7863/ultra.15.07012]

43   **Ishizaka K**, Nishida M, Motomiya M, Satoh M, Inoue M, Kudoh Y, Omotehara S, Horie T, Funakoshi T, Iwasaki N. Reliability of peripheral intraneural microhemodynamics evaluation by using contrast-enhanced ultrasonography. *J Med Ultrason (2001)* 2014; **41**: 481-486 [PMID: 27278029 DOI: 10.1007/s10396-014-0533-0]

44   **Wang Y**, Tang P, Zhang L, Wan W, He C, Tang J. Gray-scale contrast-enhanced ultrasonography for quantitative evaluation of the blood perfusion of the sciatic nerves with crush injury. *Acad Radiol* 2011; **18**: 1285-1291 [PMID: 21784669 DOI: 10.1016/j.acra.2011.06.001]

45   **Pedro MT**, Antoniadis G, Scheuerle A, Pham M, Wirtz CR, Koenig RW. Intraoperative high-resolution ultrasound and contrast-enhanced ultrasound of peripheral nerve tumors and tumorlike lesions. *Neurosurg Focus* 2015; **39**: E5 [PMID: 26323823 DOI: 10.3171/2015.6.FOCUS15218]

46   **Motomiya M**, Funakoshi T, Iwasaki N. Intraneural microvascular patterns of the median nerve assessed using contrast-enhanced ultrasonography in carpal tunnel syndrome. *J Hand Surg Eur Vol* 2016; **41**: 229-231 [PMID: 25670686 DOI: 10.1177/1753193415570222]

47   **Wang Y**, Tang P, Zhang L, Guo Y, Wan W. Quantitative evaluation of the peripheral nerve blood perfusion with high frequency contrast-enhanced ultrasound. *Acad Radiol* 2010; **17**: 1492-1497 [PMID: 20926318 DOI: 10.1016/j.acra.2010.07.007]

48   **Wei K**, Mulvagh SL, Carson L, Davidoff R, Gabriel R, Grimm RA, Wilson S, Fane L, Herzog CA, Zoghbi WA, Taylor R, Farrar M, Chaudhry FA, Porter TR, Irani W, Lang RM. The safety of deFinity and Optison for ultrasound image enhancement: a retrospective analysis of 78,383 administered contrast doses. *J Am Soc Echocardiogr* 2008; **21**: 1202-1206 [PMID: 18848430 DOI: 10.1016/j.echo.2008.07.019]

49   **Borire AA**, Issar T, Kwai NC, Visser LH, Simon NG, Poynten AM, Kiernan MC, Krishnan AV. Sonographic assessment of nerve blood flow in diabetic neuropathy. *Diabet Med* 2020; **37**: 343-349 [PMID: 31338857 DOI: 10.1111/dme.14085]

50   **Borire AA**, Arnold R, Pussell BA, Kwai NC, Visser LH, Simon NG, Kiernan MC, Krishnan AV. Effects of hemodialysis on intraneural blood flow in end-stage kidney disease. *Muscle Nerve* 2018; **57**: 287-293 [PMID: 28556350 DOI: 10.1002/mus.25704]

51   **Wee TC**, Simon NG. Ultrasound elastography for the evaluation of peripheral nerves: A systematic review. *Muscle Nerve* 2019; **60**: 501-512 [PMID: 31269240 DOI: 10.1002/mus.26624]

52   **Martin MJ**, Cartwright MS. A Pilot Study of Strain Elastography in the Diagnosis of Carpal Tunnel Syndrome. *J Clin Neurophysiol* 2017; **34**: 114-118 [PMID: 27560304 DOI: 10.1097/WNP.0000000000000334]

53   **Cingoz M**, Kandemirli SG, Alis DC, Samanci C, Kandemirli GC, Adatepe NU. Evaluation of median nerve by shear wave elastography and diffusion tensor imaging in carpal tunnel syndrome. *Eur J Radiol* 2018; **101**: 59-64 [PMID: 29571802 DOI: 10.1016/j.ejrad.2018.02.005]

54   **Zhang C**, Li M, Jiang J, Zhou Q, Xiang L, Huang Y, Ban W, Peng W. Diagnostic Value of Virtual Touch Tissue Imaging Quantification for Evaluating Median Nerve Stiffness in Carpal Tunnel Syndrome. *J Ultrasound Med* 2017; **36**: 1783-1791 [PMID: 28436592 DOI: 10.1002/jum.14213]

55   **Arslan H**, Yavuz A, İlgen F, Aycan A, Ozgokce M, Akdeniz H, Batur A. The efficiency of acoustic radiation force impulse (ARFI) elastography in the diagnosis and staging of carpal tunnel syndrome. *J Med Ultrason (2001)* 2018; **45**: 453-459 [PMID: 29330689 DOI: 10.1007/s10396-017-0857-7]

56   **Kantarci F**, Ustabasioglu FE, Delil S, Olgun DC, Korkmazer B, Dikici AS, Tutar O, Nalbantoglu M, Uzun N, Mihmanli I. Median nerve stiffness measurement by shear wave elastography: a potential sonographic method in the diagnosis of carpal tunnel syndrome. *Eur Radiol* 2014; **24**: 434-440 [PMID: 24220753 DOI: 10.1007/s00330-013-3023-7]

57   **Paluch Ł**, Pietruski P, Walecki J, Noszczyk BH. Wrist to forearm ratio as a median nerve shear wave elastography test in carpal tunnel syndrome diagnosis. *J Plast Reconstr Aesthet Surg* 2018; **71**: 1146-1152 [PMID: 29759950 DOI: 10.1016/j.bjps.2018.03.022]

58   **Yoshii Y**, Tung WL, Ishii T. Measurement of Median Nerve Strain and Applied Pressure for the Diagnosis of Carpal Tunnel Syndrome. *Ultrasound Med Biol* 2017; **43**: 1205-1209 [PMID: 28395966 DOI: 10.1016/j.ultrasmedbio.2017.02.018]

59   **Tatar IG**, Kurt A, Yavasoglu NG, Hekimoglu B. Carpal tunnel syndrome: elastosonographic strain ratio and cross-sectional area evaluation for the diagnosis and disease severity. *Med Ultrason* 2016; **18**: 305-311 [PMID: 27622406 DOI: 10.11152/mu.2013.2066.183.tat]

60   **Simon NG**, Kiernan MC. Diaphragm ultrasound in amyotrophic lateral sclerosis and other neuromuscular disorders. *Clin Neurophysiol* 2016; **127**: 28-30 [PMID: 25971722 DOI: 10.1016/j.clinph.2015.04.066]

61   **Boon AJ**, Sekiguchi H, Harper CJ, Strommen JA, Ghahfarokhi LS, Watson JC, Sorenson EJ. Sensitivity and specificity of diagnostic ultrasound in the diagnosis of phrenic neuropathy. *Neurology* 2014; **83**: 1264-1270 [PMID: 25165390 DOI: 10.1212/WNL.0000000000000841]

62   **Boon AJ**, O'Gorman C. Ultrasound in the Assessment of Respiration. *J Clin Neurophysiol* 2016; **33**: 112-119 [PMID: 27035251 DOI: 10.1097/WNP.0000000000000240]

63   **Sheppard DG**, Iyer RB, Fenstermacher MJ. Brachial plexus: demonstration at US. *Radiology* 1998; **208**: 402-406 [PMID: 9680567 DOI: 10.1148/radiology.208.2.9680567]

64   **Suk JI**, Walker FO, Cartwright MS. Ultrasonography of peripheral nerves. *Curr Neurol Neurosci Rep* 2013; **13**: 328 [PMID: 23314937 DOI: 10.1007/s11910-012-0328-x]

65   **Mallouhi A**, Pülzl P, Trieb T, Piza H, Bodner G. Predictors of carpal tunnel syndrome: accuracy of gray-scale and color Doppler sonography. *AJR Am J Roentgenol* 2006; **186**: 1240-1245 [PMID: 16632712 DOI: 10.2214/ajr.04.1715]

66   **Gonzalez NL**, Hobson-Webb LD. Neuromuscular ultrasound in clinical practice: A review. *Clin Neurophysiol Pract* 2019; **4**: 148-163 [PMID: 31886438 DOI: 10.1016/j.cnp.2019.04.006]

67   **Padua L**, Liotta G, Di Pasquale A, Granata G, Pazzaglia C, Caliandro P, Martinoli C. Contribution of ultrasound in the assessment of nerve diseases. *Eur J Neurol* 2012; **19**: 47-54 [PMID: 21554493 DOI:

10.1111/j.1468-1331.2011.03421.x]

68   **Hobson-Webb LD**, Massey JM, Juel VC, Sanders DB. The ultrasonographic wrist-to-forearm median nerve area ratio in carpal tunnel syndrome. *Clin Neurophysiol* 2008; **119**: 1353-1357 [PMID: 18387336 DOI: 10.1016/j.clinph.2008.01.101]

69   **Nakamichi K**, Tachibana S. Ultrasonographic measurement of median nerve cross-sectional area in idiopathic carpal tunnel syndrome: Diagnostic accuracy. *Muscle Nerve* 2002; **26**: 798-803 [PMID: 12451604 DOI: 10.1002/mus.10276]

70   **Wong SM**, Griffith JF, Hui AC, Lo SK, Fu M, Wong KS. Carpal tunnel syndrome: diagnostic usefulness of sonography. *Radiology* 2004; **232**: 93-99 [PMID: 15155897 DOI: 10.1148/radiol.2321030071]

71   **Mohammadi A**, Afshar A, Etemadi A, Masoudi S, Baghizadeh A. Diagnostic value of cross-sectional area of median nerve in grading severity of carpal tunnel syndrome. *Arch Iran Med* 2010; **13**: 516-521 [PMID: 21039008]

72   **Tai TW**, Wu CY, Su FC, Chern TC, Jou IM. Ultrasonography for diagnosing carpal tunnel syndrome: a meta-analysis of diagnostic test accuracy. *Ultrasound Med Biol* 2012; **38**: 1121-1128 [PMID: 22542258 DOI: 10.1016/j.ultrasmedbio.2012.02.026]

73   **Fowler JR**, Munsch M, Tosti R, Hagberg WC, Imbriglia JE. Comparison of ultrasound and electrodiagnostic testing for diagnosis of carpal tunnel syndrome: study using a validated clinical tool as the reference standard. *J Bone Joint Surg Am* 2014; **96**: e148 [PMID: 25187592 DOI: 10.2106/JBJS.M.01250]

74   **Cartwright MS**, Hobson-Webb LD, Boon AJ, Alter KE, Hunt CH, Flores VH, Werner RA, Shook SJ, Thomas TD, Primack SJ, Walker FO; American Association of Neuromuscular and Electrodiagnostic Medicine. Evidence-based guideline: neuromuscular ultrasound for the diagnosis of carpal tunnel syndrome. *Muscle Nerve* 2012; **46**: 287-293 [PMID: 22806381 DOI: 10.1002/mus.23389]

75   **Paliwal PR**, Therimadasamy AK, Chan YC, Wilder-Smith EP. Does measuring the median nerve at the carpal tunnel outlet improve ultrasound CTS diagnosis? *J Neurol Sci* 2014; **339**: 47-51 [PMID: 24485910 DOI: 10.1016/j.jns.2014.01.018]

76   **Csillik A**, Bereczki D, Bora L, Arányi Z. The significance of ultrasonographic carpal tunnel outlet measurements in the diagnosis of carpal tunnel syndrome. *Clin Neurophysiol* 2016; **127**: 3516-3523 [PMID: 27815975 DOI: 10.1016/j.clinph.2016.09.015]

77   **Sernik RA**, Abicalaf CA, Pimentel BF, Braga-Baiak A, Braga L, Cerri GG. Ultrasound features of carpal tunnel syndrome: a prospective case-control study. *Skeletal Radiol* 2008; **37**: 49-53 [PMID: 17989976 DOI: 10.1007/s00256-007-0372-9]

78   **Cartwright MS**, White DL, Demar S, Wiesler ER, Sarlikiotis T, Chloros GD, Yoon JS, Won SJ, Molnar JA, Defranzo AJ, Walker FO. Median nerve changes following steroid injection for carpal tunnel syndrome. *Muscle Nerve* 2011; **44**: 25-29 [PMID: 21674517 DOI: 10.1002/mus.22067]

79   **Aseem F**, Williams JW, Walker FO, Cartwright MS. Neuromuscular ultrasound in patients with carpal tunnel syndrome and normal nerve conduction studies. *Muscle Nerve* 2017; **55**: 913-915 [PMID: 27859374 DOI: 10.1002/mus.25462]

80   **Nakamichi K**, Tachibana S. Restricted motion of the median nerve in carpal tunnel syndrome. *J Hand Surg Br* 1995; **20**: 460-464 [PMID: 7594983 DOI: 10.1016/s0266-7681(05)80153-6]

81   **Hough AD**, Moore AP, Jones MP. Reduced longitudinal excursion of the median nerve in carpal tunnel syndrome. *Arch Phys Med Rehabil* 2007; **88**: 569-576 [PMID: 17466724 DOI: 10.1016/j.apmr.2007.02.015]

82   **Kuo TT**, Lee MR, Liao YY, Chen JP, Hsu YW, Yeh CK. Assessment of Median Nerve Mobility by Ultrasound Dynamic Imaging for Diagnosing Carpal Tunnel Syndrome. *PLoS One* 2016; **11**: e0147051 [PMID: 26764488 DOI: 10.1371/journal.pone.0147051]

83   **Park GY**, Kwon DR, Seok JI, Park DS, Cho HK. Usefulness of ultrasound assessment of median nerve mobility in carpal tunnel syndrome. *Acta Radiol* 2018; **59**: 1494-1499 [PMID: 29512394 DOI: 10.1177/0284185118762246]

84   **Lin CP**, Chen IJ, Chang KV, Wu WT, Özçakar L. Utility of Ultrasound Elastography in Evaluation of Carpal Tunnel Syndrome: A Systematic Review and Meta-analysis. *Ultrasound Med Biol* 2019; **45**: 2855-2865 [PMID: 31402226 DOI: 10.1016/j.ultrasmedbio.2019.07.409]

85   **Wee TC**, Simon NG. Shearwave Elastography in the Differentiation of Carpal Tunnel Syndrome Severity. *PM R* 2020; Epub ahead of print [PMID: 31994817 DOI: 10.1002/pmrj.12334]

86   **Yoshii Y**, Tung WL, Ishii T. Strain and Morphological Changes of Median Nerve After Carpal Tunnel Release. *J Ultrasound Med* 2017; **36**: 1153-1159 [PMID: 28240782 DOI: 10.7863/ultra.16.06070]

87   **Asadov R**, Erdal A, Buğdaycı O, Gündüz OH, Ekinci G. The effectiveness of ultrasonography and ultrasonographic elastography in the diagnosis of carpal tunnel syndrome and evaluation of treatment response after steroid injection. *Eur J Radiol* 2018; **108**: 172-176 [PMID: 30396651 DOI: 10.1016/j.ejrad.2018.09.027]

88   **Billakota S**, Hobson-Webb LD. Standard median nerve ultrasound in carpal tunnel syndrome: A retrospective review of 1,021 cases. *Clin Neurophysiol Pract* 2017; **2**: 188-191 [PMID: 30214994 DOI: 10.1016/j.cnp.2017.07.004]

89   **Bayrak IK**, Bayrak AO, Kale M, Turker H, Diren B. Bifid median nerve in patients with carpal tunnel syndrome. *J Ultrasound Med* 2008; **27**: 1129-1136 [PMID: 18645070 DOI: 10.7863/jum.2008.27.8.1129]

90   **Walker FO**, Cartwright MS, Blocker JN, Arcury TA, Suk JI, Chen H, Schulz MR, Grzywacz JG, Mora DC, Quandt SA. Prevalence of bifid median nerves and persistent median arteries and their association with carpal tunnel syndrome in a sample of Latino poultry processors and other manual workers. *Muscle Nerve* 2013; **48**: 539-544 [PMID: 24037717 DOI: 10.1002/mus.23797]

91   **Cartwright MS**, Walker FO, Newman JC, Arcury TA, Mora DC, Haiying C, Quandt SA. Muscle intrusion as a potential cause of carpal tunnel syndrome. *Muscle Nerve* 2014; **50**: 517-522 [PMID: 24449488 DOI: 10.1002/mus.24183]

92   **Beekman R**, Visser LH, Verhagen WI. Ultrasonography in ulnar neuropathy at the elbow: a critical review. *Muscle Nerve* 2011; **43**: 627-635 [PMID: 21484821 DOI: 10.1002/mus.22019]

93   **Beekman R**, Schoemaker MC, Van Der Plas JP, Van Den Berg LH, Franssen H, Wokke JH, Uitdehaag BM, Visser LH. Diagnostic value of high-resolution sonography in ulnar neuropathy at the elbow. *Neurology* 2004; **62**: 767-773 [PMID: 15007128 DOI: 10.1212/01.wnl.0000113733.62689.0d]

94   **Ozturk E**, Sonmez G, Colak A, Sildiroglu HO, Mutlu H, Senol MG, Basekim CC, Kizilkaya E. Sonographic appearances of the normal ulnar nerve in the cubital tunnel. *J Clin Ultrasound* 2008; **36**: 325-329 [PMID: 18446864 DOI: 10.1002/jcu.20486]

95   **Bayrak AO**, Bayrak IK, Turker H, Elmali M, Nural MS. Ultrasonography in patients with ulnar

neuropathy at the elbow: comparison of cross-sectional area and swelling ratio with electrophysiological severity. *Muscle Nerve* 2010; **41**: 661-666 [PMID: 19941341 DOI: 10.1002/mus.21563]

96   **Pompe SM**, Beekman R. Which ultrasonographic measure has the upper hand in ulnar neuropathy at the elbow? *Clin Neurophysiol* 2013; **124**: 190-196 [PMID: 23036180 DOI: 10.1016/j.clinph.2012.05.030]

97   **Rayegani SM**, Raeissadat SA, Kargozar E, Rahimi-Dehgolan S, Loni E. Diagnostic value of ultrasonography versus electrodiagnosis in ulnar neuropathy. *Med Devices (Auckl)* 2019; **12**: 81-88 [PMID: 30863191 DOI: 10.2147/MDER.S196106]

98   **Simon NG**, Ralph JW, Poncelet AN, Engstrom JW, Chin C, Kliot M. A comparison of ultrasonographic and electrophysiologic 'inching' in ulnar neuropathy at the elbow. *Clin Neurophysiol* 2015; **126**: 391-398 [PMID: 24962009 DOI: 10.1016/j.clinph.2014.05.023]

99   **Yoon JS**, Walker FO, Cartwright MS. Ultrasonographic swelling ratio in the diagnosis of ulnar neuropathy at the elbow. *Muscle Nerve* 2008; **38**: 1231-1235 [PMID: 18785184 DOI: 10.1002/mus.21094]

100   **Frijlink DW**, Brekelmans GJ, Visser LH. Increased nerve vascularization detected by color Doppler sonography in patients with ulnar neuropathy at the elbow indicates axonal damage. *Muscle Nerve* 2013; **47**: 188-193 [PMID: 23168608 DOI: 10.1002/mus.23505]

101   **Agarwal A**, Chandra A, Jaipal U, Saini N. Imaging in the diagnosis of ulnar nerve pathologies-a neoteric approach. *Insights Imaging* 2019; **10**: 37 [PMID: 30895491 DOI: 10.1186/s13244-019-0714-x]

102   **Sivak WN**, Hagerty SE, Huyhn L, Jordan AC, Munin MC, Spiess AM. Diagnosis of Ulnar Nerve Entrapment at the Arcade of Struthers with Electromyography and Ultrasound. *Plast Reconstr Surg Glob Open* 2016; **4**: e648 [PMID: 27257578 DOI: 10.1097/GOX.0000000000000628]

103   **Vanderpool DW**, Chalmers J, Lamb DW, Whiston TB. Peripheral compression lesions of the ulnar nerve. *J Bone Joint Surg Br* 1968; **50**: 792-803 [PMID: 4303276 DOI: 10.1302/0301-620X.50B4.792]

104   **Swenson JD**, Hutchinson DT, Bromberg M, Pace NL. Rapid onset of ulnar nerve dysfunction during transient occlusion of the brachial artery. *Anesth Analg* 1998; **87**: 677-680 [PMID: 9728852 DOI: 10.1097/00000539-199809000-00035]

105   **Chang C**, Shen M. Mononeuropathy multiplex in hemophilia: an electrophysiologic assessment. *Eur Neurol* 1998; **40**: 15-18 [PMID: 9693226 DOI: 10.1159/000007949]

106   **Masoorli S**, Angeles T, Barbone M. Danger points. How to prevent nerve injuries from venipuncture. *Nursing* 1998; **28**: 34-9; quiz 40 [PMID: 9775880 DOI: 10.1097/00152193-199809000-00016]

107   **Marin R**, McMillian D. Ulnar neuropathy associated with subdermal contraceptive implant. *South Med J* 1998; **91**: 875-878 [PMID: 9743065 DOI: 10.1097/00007611-199809000-00017]

108   **Nakamichi K**, Tachibana S, Kitajima I. Ultrasonography in the diagnosis of ulnar tunnel syndrome caused by an occult ganglion. *J Hand Surg Br* 2000; **25**: 503-504 [PMID: 10991823 DOI: 10.1054/jhsb.2000.0405]

109   **Puig S**, Turkof E, Sedivy R, Ciovica R, Lang S, Kainberger FM. Sonographic diagnosis of recurrent ulnar nerve compression by ganglion cysts. *J Ultrasound Med* 1999; **18**: 433-436 [PMID: 10361850 DOI: 10.7863/jum.1999.18.6.433]

110   **Okamoto M**, Abe M, Shirai H, Ueda N. Diagnostic ultrasonography of the ulnar nerve in cubital tunnel syndrome. *J Hand Surg Br* 2000; **25**: 499-502 [PMID: 10991822 DOI: 10.1054/jhsb.1999.0350]

111   **Lee SU**, Kim MW, Kim JM. Ultrasound Diagnosis of Double Crush Syndrome of the Ulnar Nerve by the Anconeus Epitrochlearis and a Ganglion. *J Korean Neurosurg Soc* 2016; **59**: 75-77 [PMID: 26885291 DOI: 10.3340/jkns.2016.59.1.75]

112   **Mobbs RJ**, Phan K, Maharaj MM, Chaganti J, Simon N. Intraneural Ganglion Cyst of the Ulnar Nerve at the Elbow Masquerading as a Malignant Peripheral Nerve Sheath Tumor. *World Neurosurg* 2016; **96**: 613.e5-613.e8 [PMID: 27593718 DOI: 10.1016/j.wneu.2016.08.106]

113   **Simon NG**. Treatment of ulnar neuropathy at the elbow - An ongoing conundrum. *Clin Neurophysiol* 2018; **129**: 1716-1717 [PMID: 29934265 DOI: 10.1016/j.clinph.2018.06.006]

114   **Omejec G**, Podnar S. What causes ulnar neuropathy at the elbow? *Clin Neurophysiol* 2016; **127**: 919-924 [PMID: 26093933 DOI: 10.1016/j.clinph.2015.05.027]

115   **Kim Y**, Ha DH, Lee SM. Ultrasonographic findings of posterior interosseous nerve syndrome. *Ultrasonography* 2017; **36**: 363-369 [PMID: 28494524 DOI: 10.14366/usg.17007]

116   **Dietz AR**, Bucelli RC, Pestronk A, Zaidman CM. Nerve ultrasound identifies abnormalities in the posterior interosseous nerve in patients with proximal radial neuropathies. *Muscle Nerve* 2016; **53**: 379-383 [PMID: 26201950 DOI: 10.1002/mus.24778]

117   **Djurdjevic T**, Loizides A, Löscher W, Gruber H, Plaikner M, Peer S. High resolution ultrasound in posterior interosseous nerve syndrome. *Muscle Nerve* 2014; **49**: 35-39 [PMID: 23559033 DOI: 10.1002/mus.23867]

118   **Kerasnoudis A**, Tsivgoulis G. Nerve Ultrasound in Peripheral Neuropathies: A Review. *J Neuroimaging* 2015; **25**: 528-538 [PMID: 25996962 DOI: 10.1111/jon.12261]

119   **Lo YL**, Fook-Chong S, Leoh TH, Dan YF, Tan YE, Lau WH, Chan LL. High-resolution ultrasound as a diagnostic adjunct in common peroneal neuropathy. *Arch Neurol* 2007; **64**: 1798-1800 [PMID: 18071050 DOI: 10.1001/archneur.64.12.1798]

120   **Visser LH**, Hens V, Soethout M, De Deugd-Maria V, Pijnenburg J, Brekelmans GJ. Diagnostic value of high-resolution sonography in common fibular neuropathy at the fibular head. *Muscle Nerve* 2013; **48**: 171-178 [PMID: 23801382 DOI: 10.1002/mus.23729]

121   **Bayrak İK**, Oytun Bayrak A, Türker H, Akpınar ÇK, Bolat N. Diagnostic value of ultrasonography in peroneal neuropathy. *Turk J Med Sci* 2018; **48**: 1115-1120 [PMID: 30541235 DOI: 10.3906/sag-1803-145]

122   **Kim JY**, Song S, Park HJ, Rhee WI, Won SJ. Diagnostic Cutoff Value for Ultrasonography of the Common Fibular Neuropathy at the Fibular Head. *Ann Rehabil Med* 2016; **40**: 1057-1063 [PMID: 28119836 DOI: 10.5535/arm.2016.40.6.1057]

123   **Tsukamoto H**, Granata G, Coraci D, Paolasso I, Padua L. Ultrasound and neurophysiological correlation in common fibular nerve conduction block at fibular head. *Clin Neurophysiol* 2014; **125**: 1491-1495 [PMID: 24461795 DOI: 10.1016/j.clinph.2013.11.041]

124   **Lee H**, Brekelmans GJF, Visser LH. Quantitative assessment of nerve echogenicity as an additional tool for evaluation of common fibular neuropathy. *Clin Neurophysiol* 2016; **127**: 874-879 [PMID: 25921024 DOI: 10.1016/j.clinph.2015.03.019]

125   **Bignotti B**, Assini A, Signori A, Martinoli C, Tagliafico A. Ultrasound versus MRI in common fibular neuropathy. *Muscle Nerve* 2017; **55**: 849-857 [PMID: 27668978 DOI: 10.1002/mus.25418]

126   **Visser LH**. High-resolution sonography of the common peroneal nerve: detection of intraneural ganglia. *Neurology* 2006; **67**: 1473-1475 [PMID: 17060577 DOI: 10.1212/01.wnl.0000240070.98910.bc]

127   **Grant TH**, Omar IM, Dumanian GA, Pomeranz CB, Lewis VA. Sonographic evaluation of common

peroneal neuropathy in patients with foot drop. *J Ultrasound Med* 2015; **34**: 705-711 [PMID: 25792587 DOI: 10.7863/ultra.34.4.705]

128 **Stewart JD**. Foot drop: where, why and what to do? *Pract Neurol* 2008; **8**: 158-169 [PMID: 18502948 DOI: 10.1136/jnnp.2008.149393]

129 **Aravindakannan T**, Wilder-Smith EP. High-resolution ultrasonography in the assessment of meralgia paresthetica. *Muscle Nerve* 2012; **45**: 434-435 [PMID: 22334181 DOI: 10.1002/mus.22328]

130 **Suh DH**, Kim DH, Park JW, Park BK. Sonographic and electrophysiologic findings in patients with meralgia paresthetica. *Clin Neurophysiol* 2013; **124**: 1460-1464 [PMID: 23474056 DOI: 10.1016/j.clinph.2013.02.003]

131 **Damarey B**, Demondion X, Boutry N, Kim HJ, Wavreille G, Cotten A. Sonographic assessment of the lateral femoral cutaneous nerve. *J Clin Ultrasound* 2009; **37**: 89-95 [PMID: 18803312 DOI: 10.1002/jcu.20521]

132 **Moritz T**, Prosch H, Berzaczy D, Happak W, Lieba-Samal D, Bernathova M, Auff E, Bodner G. Common anatomical variation in patients with idiopathic meralgia paresthetica: a high resolution ultrasound case-control study. *Pain Physician* 2013; **16**: E287-E293 [PMID: 23703427]

133 **Palamar D**, Terlemez R, Akgun K. Ultrasound-Guided Diagnosis and Injection of the Lateral Femoral Cutaneous Nerve with an Anatomical Variation. *Pain Pract* 2017; **17**: 1105-1108 [PMID: 28112483 DOI: 10.1111/papr.12559]

134 **Tawfik EA**, El Zohiery AK, Abouelela AA. Proposed Sonographic Criteria for the Diagnosis of Idiopathic Tarsal Tunnel Syndrome. *Arch Phys Med Rehabil* 2016; **97**: 1093-1099 [PMID: 26705883 DOI: 10.1016/j.apmr.2015.11.012]

135 **Therimadasamy AK**, Seet RC, Kagda YH, Wilder-Smith EP. Combination of ultrasound and nerve conduction studies in the diagnosis of tarsal tunnel syndrome. *Neurol India* 2011; **59**: 296-297 [PMID: 21483139 DOI: 10.4103/0028-3886.79152]

136 **Fantino O**, Coillard JY, Borne J, Bordet B. [Ultrasound of the tarsal tunnel: Normal and pathological imaging features]. *J Radiol* 2011; **92**: 1072-1080 [PMID: 22153039 DOI: 10.1016/j.jradio.2011.03.026]

137 **Samarawickrama D**, Therimadasamy AK, Chan YC, Vijayan J, Wilder-Smith EP. Nerve ultrasound in electrophysiologically verified tarsal tunnel syndrome. *Muscle Nerve* 2016; **53**: 906-912 [PMID: 26562220 DOI: 10.1002/mus.24963]

138 **Nagaoka M**, Matsuzaki H. Ultrasonography in tarsal tunnel syndrome. *J Ultrasound Med* 2005; **24**: 1035-1040 [PMID: 16040816 DOI: 10.7863/jum.2005.24.8.1035]

139 **Wu WT**, Chang KV, Özçakar L. Ultrasound facilitates the diagnosis of tarsal tunnel syndrome: intraneural ganglion cyst of the tibial nerve. *J Ultrasound* 2019; **22**: 95-98 [PMID: 30019288 DOI: 10.1007/s40477-018-0314-5]

140 **Neary KC**, Chang E, Kreulen C, Giza E. Tarsal Tunnel Syndrome Secondary to Accessory Musculature: A Case Report. *Foot Ankle Spec* 2019; **12**: 549-554 [PMID: 31409132 DOI: 10.1177/1938640019863277]

141 **Williams EH**, Rosson GD, Hagan RR, Hashemi SS, Dellon AL. Soleal sling syndrome (proximal tibial nerve compression): results of surgical decompression. *Plast Reconstr Surg* 2012; **129**: 454-462 [PMID: 21987046 DOI: 10.1097/PRS.0b013e31823aeb21]

142 **Williams EH**, Williams CG, Rosson GD, Dellon LA. Anatomic site for proximal tibial nerve compression: a cadaver study. *Ann Plast Surg* 2009; **62**: 322-325 [PMID: 19240533 DOI: 10.1097/SAP.0b013e31817e9d81]

143 **Sanchez JE**, Conkling N, Labropoulos N. Compression syndromes of the popliteal neurovascular bundle due to Baker cyst. *J Vasc Surg* 2011; **54**: 1821-1829 [PMID: 21958564 DOI: 10.1016/j.jvs.2011.07.079]

144 **Arányi Z**, Csillik A, Böhm J, Schelle T. Ultrasonographic Identification of Fibromuscular Bands Associated with Neurogenic Thoracic Outlet Syndrome: The "Wedge-Sickle" Sign. *Ultrasound Med Biol* 2016; **42**: 2357-2366 [PMID: 27444863 DOI: 10.1016/j.ultrasmedbio.2016.06.005]

145 **Leonhard V**, Caldwell G, Goh M, Reeder S, Smith HF. Ultrasonographic Diagnosis of Thoracic Outlet Syndrome Secondary to Brachial Plexus Piercing Variation. *Diagnostics (Basel)* 2017; **7**: 40 [PMID: 28677632 DOI: 10.3390/diagnostics7030040]

146 **Wadhwani R**, Chaubal N, Sukthankar R, Shroff M, Agarwala S. Color Doppler and duplex sonography in 5 patients with thoracic outlet syndrome. *J Ultrasound Med* 2001; **20**: 795-801 [PMID: 11444739 DOI: 10.7863/jum.2001.20.7.795]

147 **Simon NG**, Ralph JW, Chin C, Kliot M. Sonographic diagnosis of true neurogenic thoracic outlet syndrome. *Neurology* 2013; **81**: 1965 [PMID: 24276334 DOI: 10.1212/01.wnl.0000436621.33155.ed]

148 **Heinemeyer O**, Reimers CD. Ultrasound of radial, ulnar, median, and sciatic nerves in healthy subjects and patients with hereditary motor and sensory neuropathies. *Ultrasound Med Biol* 1999; **25**: 481-485 [PMID: 10374990 DOI: 10.1016/s0301-5629(98)00187-2]

149 **Zanette G**, Fabrizi GM, Taioli F, Lauriola MF, Badari A, Ferrarini M, Cavallaro T, Tamburin S. Nerve ultrasound findings differentiate Charcot-Marie-Tooth disease (CMT) 1A from other demyelinating CMTs. *Clin Neurophysiol* 2018; **129**: 2259-2267 [PMID: 30216910 DOI: 10.1016/j.clinph.2018.08.016]

150 **Schreiber S**, Oldag A, Kornblum C, Kollewe K, Kropf S, Schoenfeld A, Feistner H, Jakubiczka S, Kunz WS, Scherlach C, Tempelmann C, Mawrin C, Dengler R, Schreiber F, Goertler M, Vielhaber S. Sonography of the median nerve in CMT1A, CMT2A, CMTX, and HNPP. *Muscle Nerve* 2013; **47**: 385-395 [PMID: 23381770 DOI: 10.1002/mus.23681]

151 **Goedee SH**, Brekelmans GJ, van den Berg LH, Visser LH. Distinctive patterns of sonographic nerve enlargement in Charcot-Marie-Tooth type 1A and hereditary neuropathy with pressure palsies. *Clin Neurophysiol* 2015; **126**: 1413-1420 [PMID: 25454274 DOI: 10.1016/j.clinph.2014.08.026]

152 **Zaidman CM**, Harms MB, Pestronk A. Ultrasound of inherited vs. acquired demyelinating polyneuropathies. *J Neurol* 2013; **260**: 3115-3121 [PMID: 24101129 DOI: 10.1007/s00415-013-7123-8]

153 **Noto Y**, Shiga K, Tsuji Y, Mizuta I, Higuchi Y, Hashiguchi A, Takashima H, Nakagawa M, Mizuno T. Nerve ultrasound depicts peripheral nerve enlargement in patients with genetically distinct Charcot-Marie-Tooth disease. *J Neurol Neurosurg Psychiatry* 2015; **86**: 378-384 [PMID: 25091364 DOI: 10.1136/jnnp-2014-308211]

154 **Pazzaglia C**, Minciotti I, Coraci D, Briani C, Padua L. Ultrasound assessment of sural nerve in Charcot-Marie-Tooth 1A neuropathy. *Clin Neurophysiol* 2013; **124**: 1695-1699 [PMID: 23669651 DOI: 10.1016/j.clinph.2013.02.020]

155 **Padua L**, Coraci D, Lucchetta M, Paolasso I, Pazzaglia C, Granata G, Cacciavillani M, Luigetti M, Manganelli F, Pisciotta C, Piscosquito G, Pareyson D, Briani C. Different nerve ultrasound patterns in charcot-marie-tooth types and hereditary neuropathy with liability to pressure palsies. *Muscle Nerve* 2018; **57**: E18-E23 [PMID: 28802056 DOI: 10.1002/mus.25766]

156 **Cartwright MS**, Brown ME, Eulitt P, Walker FO, Lawson VH, Caress JB. Diagnostic nerve ultrasound in Charcot-Marie-Tooth disease type 1B. *Muscle Nerve* 2009; **40**: 98-102 [PMID: 19533637 DOI: 10.1002/mus.21292]

157 **Carroll AS**, Burns J, Nicholson G, Kiernan MC, Vucic S. Inherited Neuropathies. *Semin Neurol* 2019; **39**: 620-639 [PMID: 31639845 DOI: 10.1055/s-0039-1693006]

158 **Fabrizi GM**, Tamburin S, Cavallaro T, Cabrini I, Ferrarini M, Taioli F, Magrinelli F, Zanette G. The spectrum of Charcot-Marie-Tooth disease due to myelin protein zero: An electrodiagnostic, nerve ultrasound and histological study. *Clin Neurophysiol* 2018; **129**: 21-32 [PMID: 29136549 DOI: 10.1016/j.clinph.2017.09.117]

159 **Grimm A**, Rasenack M, Athanasopoulou IM, Dammeier NM, Lipski C, Wolking S, Vittore D, Décard BF, Axer H. The modified ultrasound pattern sum score mUPSS as additional diagnostic tool for genetically distinct hereditary neuropathies. *J Neurol* 2016; **263**: 221-230 [PMID: 26559821 DOI: 10.1007/s00415-015-7953-7]

160 **Vallat JM**, Ouvrier RA, Pollard JD, Magdelaine C, Zhu D, Nicholson GA, Grew S, Ryan MM, Funalot B. Histopathological findings in hereditary motor and sensory neuropathy of axonal type with onset in early childhood associated with mitofusin 2 mutations. *J Neuropathol Exp Neurol* 2008; **67**: 1097-1102 [PMID: 18957892 DOI: 10.1097/NEN.0b013e31818b6cbc]

161 **Shahrizaila N**, Noto Y, Simon NG, Huynh W, Shibuya K, Matamala JM, Dharmadasa T, Devenney E, Kennerson ML, Nicholson GA, Kiernan MC. Quantitative muscle ultrasound as a biomarker in Charcot-Marie-Tooth neuropathy. *Clin Neurophysiol* 2017; **128**: 227-232 [PMID: 27940147 DOI: 10.1016/j.clinph.2016.11.010]

162 **Bayrak AO**, Bayrak IK, Battaloglu E, Ozes B, Yildiz O, Onar MK. Ultrasonographic findings in hereditary neuropathy with liability to pressure palsies. *Neurol Res* 2015; **37**: 106-111 [PMID: 25005138 DOI: 10.1179/1743132814Y.0000000411]

163 **Hooper DR**, Lawson W, Smith L, Baker SK. Sonographic features in hereditary neuropathy with liability to pressure palsies. *Muscle Nerve* 2011; **44**: 862-867 [PMID: 22102454 DOI: 10.1002/mus.22199]

164 **Beekman R**, Visser LH. Sonographic detection of diffuse peripheral nerve enlargement in hereditary neuropathy with liability to pressure palsies. *J Clin Ultrasound* 2002; **30**: 433-436 [PMID: 12210462 DOI: 10.1002/jcu.10090]

165 **Ginanneschi F**, Filippou G, Giannini F, Carluccio MA, Adinolfi A, Frediani B, Dotti MT, Rossi A. Sonographic and electrodiagnostic features of hereditary neuropathy with liability to pressure palsies. *J Peripher Nerv Syst* 2012; **17**: 391-398 [PMID: 23279340 DOI: 10.1111/j.1529-8027.2012.00437.x]

166 **Cacciavillani M**, Padua L, Gasparotti R, Briani C. HNPP: not only entrapment sites. Ultrasound digital nerve abnormalities in a guitar player. *Neurol Sci* 2016; **37**: 999-1000 [PMID: 27056376 DOI: 10.1007/s10072-015-2449-x]

167 **Kollmer J**, Hund E, Hornung B, Hegenbart U, Schönland SO, Kimmich C, Kristen AV, Purrucker J, Röcken C, Heiland S, Bendszus M, Pham M. In vivo detection of nerve injury in familial amyloid polyneuropathy by magnetic resonance neurography. *Brain* 2015; **138**: 549-562 [PMID: 25526974 DOI: 10.1093/brain/awu344]

168 **Kollmer J**, Sahm F, Hegenbart U, Purrucker JC, Kimmich C, Schönland SO, Hund E, Heiland S, Hayes JM, Kristen AV, Röcken C, Pham M, Bendszus M, Weiler M. Sural nerve injury in familial amyloid polyneuropathy: MR neurography vs clinicopathologic tools. *Neurology* 2017; **89**: 475-484 [PMID: 28679600 DOI: 10.1212/WNL.0000000000004178]

169 **Granata G**, Luigetti M, Coraci D, Del Grande A, Romano A, Bisogni G, Bramanti P, Rossini PM, Sabatelli M, Padua L. Ultrasound evaluation in transthyretin-related amyloid neuropathy. *Muscle Nerve* 2014; **50**: 372-376 [PMID: 24395461 DOI: 10.1002/mus.24168]

170 **Podnar S**, Sarafov S, Tournev I, Omejec G, Zidar J. Peripheral nerve ultrasonography in patients with transthyretin amyloidosis. *Clin Neurophysiol* 2017; **128**: 505-511 [PMID: 28226286 DOI: 10.1016/j.clinph.2017.01.013]

171 **Cortese A**, Simone R, Sullivan R, Vandrovcova J, Tariq H, Yau WY, Humphrey J, Jaunmuktane Z, Sivakumar P, Polke J, Ilyas M, Tribollet E, Tomaselli PJ, Devigili G, Callegari I, Versino M, Salpietro V, Efthymiou S, Kaski D, Wood NW, Andrade NS, Buglo E, Rebelo A, Rossor AM, Bronstein A, Fratta P, Marques WJ, Züchner S, Reilly MM, Houlden H. Biallelic expansion of an intronic repeat in RFC1 is a common cause of late-onset ataxia. *Nat Genet* 2019; **51**: 649-658 [PMID: 30926972 DOI: 10.1038/s41588-019-0372-4]

172 **Pelosi L**, Mulroy E, Leadbetter R, Kilfoyle D, Chancellor AM, Mossman S, Wing L, Wu TY, Roxburgh RH. Peripheral nerves are pathologically small in cerebellar ataxia neuropathy vestibular areflexia syndrome: a controlled ultrasound study. *Eur J Neurol* 2018; **25**: 659-665 [PMID: 29316033 DOI: 10.1111/ene.13563]

173 **Leadbetter R**, Weatherall M, Pelosi L. Nerve ultrasound as a diagnostic tool for sensory neuronopathy in spinocerebellar ataxia syndrome. *Clin Neurophysiol* 2019; **130**: 568-572 [PMID: 30713001 DOI: 10.1016/j.clinph.2018.12.010]

174 **Szmulewicz DJ**, McLean CA, Rodriguez ML, Chancellor AM, Mossman S, Lamont D, Roberts L, Storey E, Halmagyi GM. Dorsal root ganglionopathy is responsible for the sensory impairment in CANVAS. *Neurology* 2014; **82**: 1410-1415 [PMID: 24682971 DOI: 10.1212/WNL.0000000000000352]

175 **Szmulewicz DJ**, McLean CA, MacDougall HG, Roberts L, Storey E, Halmagyi GM. CANVAS an update: clinical presentation, investigation and management. *J Vestib Res* 2014; **24**: 465-474 [PMID: 25564090 DOI: 10.3233/VES-140536]

176 **Linnemann C**, Tezenas du Montcel S, Rakowicz M, Schmitz-Hübsch T, Szymanski S, Berciano J, van de Warrenburg BP, Pedersen K, Depondt C, Rola R, Klockgether T, García A, Mutlu G, Schöls L. Peripheral Neuropathy in Spinocerebellar Ataxia Type 1, 2, 3, and 6. *Cerebellum* 2016; **15**: 165-173 [PMID: 26054379 DOI: 10.1007/s12311-015-0684-6]

177 **Velázquez-Perez L**, Rodríguez-Labrada R, Canales-Ochoa N, Sanchez-Cruz G, Fernandez-Ruiz J, Montero JM, Aguilera-Rodríguez R, Diaz R, Almaguer-Mederos LE, Truitz AP. Progression markers of Spinocerebellar ataxia 2. A twenty years neurophysiological follow up study. *J Neurol Sci* 2010; **290**: 22-26 [PMID: 20070987 DOI: 10.1016/j.jns.2009.12.013]

178 **Pelosi L**, Iodice R, Antenora A, Kilfoyle D, Mulroy E, Rodrigues M, Roxburgh R, Iovino A, Filla A, Manganelli F, Santoro L. Spinocerebellar ataxia type 2-neuronopathy or neuropathy? *Muscle Nerve* 2019; **60**: 271-278 [PMID: 31228263 DOI: 10.1002/mus.26613]

179 **Morral JA**, Davis AN, Qian J, Gelman BB, Koeppen AH. Pathology and pathogenesis of sensory neuropathy in Friedreich's ataxia. *Acta Neuropathol* 2010; **120**: 97-108 [PMID: 20339857 DOI:

10.1007/s00401-010-0675-0]

180   **Koeppen AH**, Morral JA, Davis AN, Qian J, Petrocine SV, Knutson MD, Gibson WM, Cusack MJ, Li D. The dorsal root ganglion in Friedreich's ataxia. *Acta Neuropathol* 2009; **118**: 763-776 [PMID: 19727777 DOI: 10.1007/s00401-009-0589-x]

181   **Mulroy E**, Pelosi L, Leadbetter R, Joshi P, Rodrigues M, Mossman S, Kilfoyle D, Roxburgh R. Peripheral nerve ultrasound in Friedreich ataxia. *Muscle Nerve* 2018; **57**: 852-856 [PMID: 29130498 DOI: 10.1002/mus.26012]

182   **Lu C**, Schoenfeld R, Shan Y, Tsai HJ, Hammock B, Cortopassi G. Frataxin deficiency induces Schwann cell inflammation and death. *Biochim Biophys Acta* 2009; **1792**: 1052-1061 [PMID: 19679182 DOI: 10.1016/j.bbadis.2009.07.011]

183   **Dyck PJ**, Lais AC, Ohta M, Bastron JA, Okazaki H, Groover RV. Chronic inflammatory polyradiculoneuropathy. *Mayo Clin Proc* 1975; **50**: 621-637 [PMID: 1186294]

184   **Kerasnoudis A**, Pitarokoili K, Behrendt V, Gold R, Yoon MS. Correlation of nerve ultrasound, electrophysiological and clinical findings in chronic inflammatory demyelinating polyneuropathy. *J Neuroimaging* 2015; **25**: 207-216 [PMID: 24593005 DOI: 10.1111/jon.12079]

185   **Zaidman CM**, Pestronk A. Nerve size in chronic inflammatory demyelinating neuropathy varies with disease activity and therapy response over time: a retrospective ultrasound study. *Muscle Nerve* 2014; **50**: 733-738 [PMID: 24615614 DOI: 10.1002/mus.24227]

186   **Matsuoka N**, Kohriyama T, Ochi K, Nishitani M, Sueda Y, Mimori Y, Nakamura S, Matsumoto M. Detection of cervical nerve root hypertrophy by ultrasonography in chronic inflammatory demyelinating polyradiculoneuropathy. *J Neurol Sci* 2004; **219**: 15-21 [PMID: 15050432 DOI: 10.1016/j.jns.2003.11.011]

187   **Jang JH**, Cho CS, Yang KS, Seok HY, Kim BJ. Pattern analysis of nerve enlargement using ultrasonography in chronic inflammatory demyelinating polyneuropathy. *Clin Neurophysiol* 2014; **125**: 1893-1899 [PMID: 24560630 DOI: 10.1016/j.clinph.2013.12.115]

188   **Grimm A**, Décard BF, Axer H, Fuhr P. The Ultrasound pattern sum score - UPSS. A new method to differentiate acute and subacute neuropathies using ultrasound of the peripheral nerves. *Clin Neurophysiol* 2015; **126**: 2216-2225 [PMID: 25691156 DOI: 10.1016/j.clinph.2015.01.011]

189   **Grimm A**, Heiling B, Schumacher U, Witte OW, Axer H. Ultrasound differentiation of axonal and demyelinating neuropathies. *Muscle Nerve* 2014; **50**: 976-983 [PMID: 24634226 DOI: 10.1002/mus.24238]

190   **Padua L**, Granata G, Sabatelli M, Inghilleri M, Lucchetta M, Luigetti M, Coraci D, Martinoli C, Briani C. Heterogeneity of root and nerve ultrasound pattern in CIDP patients. *Clin Neurophysiol* 2014; **125**: 160-165 [PMID: 24099922 DOI: 10.1016/j.clinph.2013.07.023]

191   **Grimm A**, Vittore D, Schubert V, Rasenack M, Décard BF, Heiling B, Hammer N, Axer H. Ultrasound aspects in therapy-naive CIDP compared to long-term treated CIDP. *J Neurol* 2016; **263**: 1074-1082 [PMID: 27017343 DOI: 10.1007/s00415-016-8100-9]

192   **Rajabally YA**, Morlese J, Kathuria D, Khan A. Median nerve ultrasonography in distinguishing neuropathy sub-types: a pilot study. *Acta Neurol Scand* 2012; **125**: 254-259 [PMID: 21615356 DOI: 10.1111/j.1600-0404.2011.01527.x]

193   **Padua L**, Martinoli C, Pazzaglia C, Lucchetta M, Granata G, Erra C, Briani C. Intra- and internerve cross-sectional area variability: new ultrasound measures. *Muscle Nerve* 2012; **45**: 730-733 [PMID: 22499101 DOI: 10.1002/mus.23252]

194   **Niu J**, Cui L, Liu M. Multiple Sites Ultrasonography of Peripheral Nerves in Differentiating Charcot-Marie-Tooth Type 1A from Chronic Inflammatory Demyelinating Polyradiculoneuropathy. *Front Neurol* 2017; **8**: 181 [PMID: 28522988 DOI: 10.3389/fneur.2017.00181]

195   **Kerasnoudis A**, Pitarokoili K, Behrendt V, Gold R, Yoon MS. Bochum ultrasound score versus clinical and electrophysiological parameters in distinguishing acute-onset chronic from acute inflammatory demyelinating polyneuropathy. *Muscle Nerve* 2015; **51**: 846-852 [PMID: 25297575 DOI: 10.1002/mus.24484]

196   **Grimm A**, Vittore D, Schubert V, Lipski C, Heiling B, Décard BF, Axer H. Ultrasound pattern sum score, homogeneity score and regional nerve enlargement index for differentiation of demyelinating inflammatory and hereditary neuropathies. *Clin Neurophysiol* 2016; **127**: 2618-2624 [PMID: 27291881 DOI: 10.1016/j.clinph.2016.04.009]

197   **Gallardo E**, Sedano MJ, Orizaola P, Sánchez-Juan P, González-Suárez A, García A, Terán-Villagrá N, Ruiz-Soto M, Álvaro RL, Berciano MT, Lafarga M, Berciano J. Spinal nerve involvement in early Guillain-Barré syndrome: a clinico-electrophysiological, ultrasonographic and pathological study. *Clin Neurophysiol* 2015; **126**: 810-819 [PMID: 25213352 DOI: 10.1016/j.clinph.2014.06.051]

198   **Grimm A**, Décard BF, Axer H. Ultrasonography of the peripheral nervous system in the early stage of Guillain-Barré syndrome. *J Peripher Nerv Syst* 2014; **19**: 234-241 [PMID: 25418824 DOI: 10.1111/jns.12091]

199   **Kerasnoudis A**, Pitarokoili K, Behrendt V, Gold R, Yoon MS. Correlation of nerve ultrasound, electrophysiological, and clinical findings in post Guillain-Barré syndrome. *J Peripher Nerv Syst* 2013; **18**: 232-240 [PMID: 24028191 DOI: 10.1111/jns5.12037]

200   **Almeida V**, Mariotti P, Veltri S, Erra C, Padua L. Nerve ultrasound follow-up in a child with Guillain-Barré syndrome. *Muscle Nerve* 2012; **46**: 270-275 [PMID: 22806378 DOI: 10.1002/mus.23325]

201   **Razali SNO**, Arumugam T, Yuki N, Rozalli FI, Goh KJ, Shahrizaila N. Serial peripheral nerve ultrasound in Guillain-Barré syndrome. *Clin Neurophysiol* 2016; **127**: 1652-1656 [PMID: 26228791 DOI: 10.1016/j.clinph.2015.06.030]

202   **Mori A**, Nodera H, Takamatsu N, Maruyama-Saladini K, Osaki Y, Shimatani Y, Kaji R. Sonographic evaluation of peripheral nerves in subtypes of Guillain-Barré syndrome. *J Neurol Sci* 2016; **364**: 154-159 [PMID: 27084237 DOI: 10.1016/j.jns.2016.03.042]

203   **Scheidl E**, Böhm J, Simó M, Rózsa C, Bereznai B, Kovács T, Arányi Z. Ultrasonography of MADSAM neuropathy: focal nerve enlargements at sites of existing and resolved conduction blocks. *Neuromuscl Disord* 2012; **22**: 627-631 [PMID: 22513319 DOI: 10.1016/j.nmd.2012.03.005]

204   **Neubauer C**, Gruber H, Bäuerle J, Egger K. Ultrasonography of Multifocal Acquired Demyelinating Sensory and Motor Neuropathy (MADSAM). *Clin Neuroradiol* 2015; **25**: 423-425 [PMID: 25556187 DOI: 10.1007/s00062-014-0364-9]

205   **Simon NG**, Kiernan MC. Precise correlation between structural and electrophysiological disturbances in MADSAM neuropathy. *Neuromuscl Disord* 2015; **25**: 904-907 [PMID: 26314279 DOI: 10.1016/j.nmd.2015.07.012]

206 **Tanaka K**, Ota N, Harada Y, Wada I, Suenaga T. Normalization of sonographical multifocal nerve enlargements in a MADSAM patient following a good clinical response to intravenous immunoglobulin. *Neuromuscul Disord* 2016; **26**: 619-623 [PMID: 27460345 DOI: 10.1016/j.nmd.2016.06.008]

207 **Grimm A**, Thomaser AL, Peters N, Fuhr P. Neurological picture. Vagal hypertrophy in immune-mediated neuropathy visualised with high-resolution ultrasound (HR-US). *J Neurol Neurosurg Psychiatry* 2015; **86**: 1277-1278 [PMID: 25209417 DOI: 10.1136/jnnp-2014-308271]

208 **Loewenbrück KF**, Liesenberg J, Dittrich M, Schäfer J, Patzner B, Trausch B, Machetanz J, Hermann A, Storch A. Nerve ultrasound in the differentiation of multifocal motor neuropathy (MMN) and amyotrophic lateral sclerosis with predominant lower motor neuron disease (ALS/LMND). *J Neurol* 2016; **263**: 35-44 [PMID: 26477025 DOI: 10.1007/s00415-015-7927-9]

209 **Grimm A**, Décard BF, Athanasopoulou I, Schweikert K, Sinnreich M, Axer H. Nerve ultrasound for differentiation between amyotrophic lateral sclerosis and multifocal motor neuropathy. *J Neurol* 2015; **262**: 870-880 [PMID: 25626722 DOI: 10.1007/s00415-015-7648-0]

210 **Beekman R**, van den Berg LH, Franssen H, Visser LH, van Asseldonk JT, Wokke JH. Ultrasonography shows extensive nerve enlargements in multifocal motor neuropathy. *Neurology* 2005; **65**: 305-307 [PMID: 16043806 DOI: 10.1212/01.wnl.0000169179.67764.30]

211 **Jongbloed BA**, Haakma W, Goedee HS, Bos JW, Bos C, Hendrikse J, Van Den Berg LH, Van Der Pol WL. Comparative study of peripheral nerve Mri and ultrasound in multifocal motor neuropathy and amyotrophic lateral sclerosis. *Muscle Nerve* 2016; **54**: 1133-1135 [PMID: 27571543 DOI: 10.1002/mus.25391]

212 **Oudeman J**, Eftimov F, Strijkers GJ, Schneiders JJ, Roosendaal SD, Engbersen MP, Froeling M, Goedee HS, van Doorn PA, Caan MWA, van Schaik IN, Maas M, Nederveen AJ, de Visser M, Verhamme C. Diagnostic accuracy of MRI and ultrasound in chronic immune-mediated neuropathies. *Neurology* 2020; **94**: e62-e74 [PMID: 31827006 DOI: 10.1212/WNL.0000000000008697]

213 **Simon NG**, Ayer G, Lomen-Hoerth C. Is IVIg therapy warranted in progressive lower motor neuron syndromes without conduction block? *Neurology* 2013; **81**: 2116-2120 [PMID: 24212395 DOI: 10.1212/01.wnl.0000437301.28441.7e]

214 **Merola A**, Rosso M, Romagnolo A, Peci E, Cocito D. Peripheral Nerve Ultrasonography in Chronic Inflammatory Demyelinating Polyradiculoneuropathy and Multifocal Motor Neuropathy: Correlations with Clinical and Neurophysiological Data. *Neurol Res Int* 2016; **2016**: 9478593 [PMID: 27313890 DOI: 10.1155/2016/9478593]

215 **Kerasnoudis A**, Pitarokoili K, Behrendt V, Gold R, Yoon MS. Multifocal motor neuropathy: correlation of nerve ultrasound, electrophysiological, and clinical findings. *J Peripher Nerv Syst* 2014; **19**: 165-174 [PMID: 24862982 DOI: 10.1111/jns5.12067]

216 **van Rosmalen M**, Lieba-Samal D, Pillen S, van Alfen N. Ultrasound of peripheral nerves in neuralgic amyotrophy. *Muscle Nerve* 2019; **59**: 55-59 [PMID: 30107038 DOI: 10.1002/mus.26322]

217 **Shen J**, Cartwright MS. Neuromuscular Ultrasound in the Assessment of Polyneuropathies and Motor Neuron Disease. *J Clin Neurophysiol* 2016; **33**: 86-93 [PMID: 27035248 DOI: 10.1097/WNP.0000000000000241]

218 **Arányi Z**, Csillik A, Dévay K, Rosero M, Barsi P, Böhm J, Schelle T. Ultrasonographic identification of nerve pathology in neuralgic amyotrophy: Enlargement, constriction, fascicular entwinement, and torsion. *Muscle Nerve* 2015; **52**: 503-511 [PMID: 25703205 DOI: 10.1002/mus.24615]

219 **ArÁnyi Z**, Csillik A, DéVay K, Rosero M, Barsi P, BÖhm J, Schelle T. Ultrasonography in neuralgic amyotrophy: Sensitivity, spectrum of findings, and clinical correlations. *Muscle Nerve* 2017; **56**: 1054-1062 [PMID: 28556181 DOI: 10.1002/mus.25708]

220 **Leupold D**, Felbecker A, Tettenborn B, Hundsberger T. Nerve Ultrasound as a Decisive Tool in Nonsystemic Vasculitic Neuropathy: A Case Report. *Case Rep Neurol* 2016; **8**: 108-114 [PMID: 27403131 DOI: 10.1159/000446314]

221 **Grimm A**, Décard BF, Bischof A, Axer H. Ultrasound of the peripheral nerves in systemic vasculitic neuropathies. *J Neurol Sci* 2014; **347**: 44-49 [PMID: 25262016 DOI: 10.1016/j.jns.2014.09.017]

222 **Goedee HS**, van der Pol WL, van Asseldonk JH, Vrancken AFJE, Notermans NC, Visser LH, van den Berg LH. Nerve sonography to detect peripheral nerve involvement in vasculitis syndromes. *Neurol Clin Pract* 2016; **6**: 293-303 [PMID: 29443128 DOI: 10.1212/CPJ.0000000000000258]

223 **Ito T**, Kijima M, Watanabe T, Sakuta M, Nishiyama K. Ultrasonography of the tibial nerve in vasculitic neuropathy. *Muscle Nerve* 2007; **35**: 379-382 [PMID: 17058270 DOI: 10.1002/mus.20673]

224 **Üçeyler N**, Schäfer KA, Mackenrodt D, Sommer C, Müllges W. High-Resolution Ultrasonography of the Superficial Peroneal Motor and Sural Sensory Nerves May Be a Non-invasive Approach to the Diagnosis of Vasculitic Neuropathy. *Front Neurol* 2016; **7**: 48 [PMID: 27064457 DOI: 10.3389/fneur.2016.00048]

225 **Lucchetta M**, Padua L, Granata G, Luigetti M, Campagnolo M, Dalla Torre C, Coraci D, Sabatelli M, Briani C. Nerve ultrasound findings in neuropathy associated with anti-myelin-associated glycoprotein antibodies. *Eur J Neurol* 2015; **22**: 193-202 [PMID: 25174585 DOI: 10.1111/ene.12554]

226 **Garg N**, Park SB, Howells J, Noto YI, Vucic S, Yiannikas C, Tomlinson SE, Huynh W, Simon NG, Mathey EK, Spies J, Pollard JD, Krishnan AV, Kiernan MC. Anti-MAG neuropathy: Role of IgM antibodies, the paranodal junction and juxtaparanodal potassium channels. *Clin Neurophysiol* 2018; **129**: 2162-2169 [PMID: 30144659 DOI: 10.1016/j.clinph.2018.07.021]

227 **Keddie S**, D'Sa S, Foldes D, Carr AS, Reilly MM, Lunn MPT. POEMS neuropathy: optimising diagnosis and management. *Pract Neurol* 2018; **18**: 278-290 [PMID: 29511110 DOI: 10.1136/practneurol-2017-001792]

228 **Lucchetta M**, Pazzaglia C, Granata G, Briani C, Padua L. Ultrasound evaluation of peripheral neuropathy in POEMS syndrome. *Muscle Nerve* 2011; **44**: 868-872 [PMID: 22102455 DOI: 10.1002/mus.22258]

229 **Piccione EA**, Engelstad J, Dyck PJ, Mauermann ML, Dispenzieri A, Dyck PJ. Nerve pathologic features differentiate POEMS syndrome from CIDP. *Acta Neuropathol Commun* 2016; **4**: 116 [PMID: 27799073 DOI: 10.1186/s40478-016-0389-1]

230 **Del Grande A**, Sabatelli M, Luigetti M, Conte A, Granata G, Rufini V, Del Ciello A, Gaudino S, Fernandez E, Hohaus S, Coli A, Lauriola L. Primary multifocal lymphoma of peripheral nervous system: case report and review of the literature. *Muscle Nerve* 2014; **50**: 1016-1022 [PMID: 25088432 DOI: 10.1002/mus.24354]

231 **Cartwright MS**, Walker FO, Griffin LP, Caress JB. Peripheral nerve and muscle ultrasound in amyotrophic lateral sclerosis. *Muscle Nerve* 2011; **44**: 346-351 [PMID: 21815172 DOI: 10.1002/mus.22035]

232 **Schreiber S**, Abdulla S, Debska-Vielhaber G, Machts J, Dannhardt-Stieger V, Feistner H, Oldag A,

Goertler M, Petri S, Kollewe K, Kropf S, Schreiber F, Heinze HJ, Dengler R, Nestor PJ, Vielhaber S. Peripheral nerve ultrasound in amyotrophic lateral sclerosis phenotypes. *Muscle Nerve* 2015; **51**: 669-675 [PMID: 25155020 DOI: 10.1002/mus.24431]

233   **Ríos-Díaz J**, Del Baño-Aledo ME, Tembl-Ferrairó JI, Chumillas MJ, Vázquez-Costa JF, Martínez-Payá JJ. Quantitative neuromuscular ultrasound analysis as biomarkers in amyotrophic lateral sclerosis. *Eur Radiol* 2019; **29**: 4266-4275 [PMID: 30666448 DOI: 10.1007/s00330-018-5943-8]

234   **Nodera H**, Takamatsu N, Shimatani Y, Mori A, Sato K, Oda M, Terasawa Y, Izumi Y, Kaji R. Thinning of cervical nerve roots and peripheral nerves in ALS as measured by sonography. *Clin Neurophysiol* 2014; **125**: 1906-1911 [PMID: 24657162 DOI: 10.1016/j.clinph.2014.01.033]

235   **Noto YI**, Garg N, Li T, Timmins HC, Park SB, Shibuya K, Shahrizaila N, Huynh W, Matamala JM, Dharmadasa T, Yiannikas C, Vucic S, Kiernan MC. Comparison of cross-sectional areas and distal-proximal nerve ratios in amyotrophic lateral sclerosis. *Muscle Nerve* 2018; **58**: 777-783 [PMID: 30019401 DOI: 10.1002/mus.26301]

236   **Pathak S**, Caress JB, Wosiski-Kuhn M, Milligan C, Williams D, Cartwright MS. A pilot study of neuromuscular ultrasound as a biomarker for amyotrophic lateral sclerosis. *Muscle Nerve* 2019; **59**: 181-186 [PMID: 30338851 DOI: 10.1002/mus.26360]

237   **Heckmatt JZ**, Leeman S, Dubowitz V. Ultrasound imaging in the diagnosis of muscle disease. *J Pediatr* 1982; **101**: 656-660 [PMID: 7131136 DOI: 10.1016/s0022-3476(82)80286-2]

238   **Arts IMP**, Overeem S, Pillen S, Jurgen Schelhaas H, Zwarts MJ. Muscle changes in amyotrophic lateral sclerosis: a longitudinal ultrasonography study. *Clin Neurophysiol* 2011; **122**: 623-628 [PMID: 20810308 DOI: 10.1016/j.clinph.2010.07.023]

239   **Misawa S**, Noto Y, Shibuya K, Isose S, Sekiguchi Y, Nasu S, Kuwabara S. Ultrasonographic detection of fasciculations markedly increases diagnostic sensitivity of ALS. *Neurology* 2011; **77**: 1532-1537 [PMID: 21940619 DOI: 10.1212/WNL.0b013e318233b36a]

240   **Johansson MT**, Ellegaard HR, Tankisi H, Fuglsang-Frederiksen A, Qerama E. Fasciculations in nerve and muscle disorders - A prospective study of muscle ultrasound compared to electromyography. *Clin Neurophysiol* 2017; **128**: 2250-2257 [PMID: 29028499 DOI: 10.1016/j.clinph.2017.08.031]

241   **Tsuji Y**, Noto YI, Shiga K, Teramukai S, Nakagawa M, Mizuno T. A muscle ultrasound score in the diagnosis of amyotrophic lateral sclerosis. *Clin Neurophysiol* 2017; **128**: 1069-1074 [PMID: 28343888 DOI: 10.1016/j.clinph.2017.02.015]

242   **Wee TC**, Simon NG. Applications of neuromuscular ultrasound in amyotrophic lateral sclerosis. *Clin Neurophysiol* 2018; **129**: 2638-2639 [PMID: 30385110 DOI: 10.1016/j.clinph.2018.10.003]

243   **Pinto S**, Alves P, Pimentel B, Swash M, de Carvalho M. Ultrasound for assessment of diaphragm in ALS. *Clin Neurophysiol* 2016; **127**: 892-897 [PMID: 25971723 DOI: 10.1016/j.clinph.2015.03.024]

244   **Fantini R**, Tonelli R, Castaniere I, Tabbì L, Pellegrino MR, Cerri S, Livrieri F, Giaroni F, Monelli M, Ruggieri V, Fini N, Mandrioli J, Clini E, Marchioni A. Serial ultrasound assessment of diaphragmatic function and clinical outcome in patients with amyotrophic lateral sclerosis. *BMC Pulm Med* 2019; **19**: 160 [PMID: 31455341 DOI: 10.1186/s12890-019-0924-5]

245   **Noto YI**, Simon N, Shibuya K, Matamala JM, Dharmadasa T, Kiernan MC. Dynamic muscle ultrasound identifies upper motor neuron involvement in amyotrophic lateral sclerosis. *Amyotroph Lateral Scler Frontotemporal Degener* 2017; **18**: 404-410 [PMID: 28613097 DOI: 10.1080/21678421.2017.1286355]

246   **Borire AA**, Issar T, Kwai NC, Visser LH, Simon NG, Poynten AM, Kiernan MC, Krishnan AV. Correlation between markers of peripheral nerve function and structure in type 1 diabetes. *Diabetes Metab Res Rev* 2018; **34**: e3028 [PMID: 29858541 DOI: 10.1002/dmrr.3028]

247   **Riazi S**, Bril V, Perkins BA, Abbas S, Chan VW, Ngo M, Lovblom LE, El-Beheiry H, Brull R. Can ultrasound of the tibial nerve detect diabetic peripheral neuropathy? A cross-sectional study. *Diabetes Care* 2012; **35**: 2575-2579 [PMID: 23033242 DOI: 10.2337/dc12-0739]

248   **Lee D**, Dauphinée DM. Morphological and functional changes in the diabetic peripheral nerve: using diagnostic ultrasound and neurosensory testing to select candidates for nerve decompression. *J Am Podiatr Med Assoc* 2005; **95**: 433-437 [PMID: 16166459 DOI: 10.7547/0950433]

249   **Singh K**, Gupta K, Kaur S. High resolution ultrasonography of the tibial nerve in diabetic peripheral neuropathy. *J Ultrason* 2017; **17**: 246-252 [PMID: 29375899 DOI: 10.15557/JoU.2017.0036]

250   **Watanabe T**, Ito H, Sekine A, Katano Y, Nishimura T, Kato Y, Takeda J, Seishima M, Matsuoka T. Sonographic evaluation of the peripheral nerve in diabetic patients: the relationship between nerve conduction studies, echo intensity, and cross-sectional area. *J Ultrasound Med* 2010; **29**: 697-708 [PMID: 20427781 DOI: 10.7863/jum.2010.29.5.697]

251   **Breiner A**, Qrimli M, Ebadi H, Alabdali M, Lovblom LE, Abraham A, Albulahi H, Perkins BA, Bril V. Peripheral nerve high-resolution ultrasound in diabetes. *Muscle Nerve* 2017; **55**: 171-178 [PMID: 27312883 DOI: 10.1002/mus.25223]

252   **Dikici AS**, Ustabasioglu FE, Delil S, Nalbantoglu M, Korkmaz B, Bakan S, Kula O, Uzun N, Mihmanli I, Kantarci F. Evaluation of the Tibial Nerve with Shear-Wave Elastography: A Potential Sonographic Method for the Diagnosis of Diabetic Peripheral Neuropathy. *Radiology* 2017; **282**: 494-501 [PMID: 27643671 DOI: 10.1148/radiol.2016160135]

253   **Briani C**, Campagnolo M, Lucchetta M, Cacciavillani M, Dalla Torre C, Granata G, Bergamo F, Lonardi S, Zagonel V, Cavaletti G, Ermani M, Padua L. Ultrasound assessment of oxaliplatin-induced neuropathy and correlations with neurophysiologic findings. *Eur J Neurol* 2013; **20**: 188-192 [PMID: 22943629 DOI: 10.1111/j.1468-1331.2012.03852.x]

254   **Lycan T**, Thomas A, Hsu F, Cartwright M, Walker F, Ahn C, Sangueza O, Shiozawa Y, Park S, Peters C, Melin S, Avery T, Sorscher S, Lesser G, Strowd R. Neuromuscular ultrasound for assessment of peripheral neuropathy in breast cancer patients receiving taxane therapy. *J Clin Oncol* 2018; **36**: e22083-e22083 [DOI: 10.1200/JCO.2018.36.15_suppl.e22083]

255   **Athanasopoulou IM**, Rasenack M, Grimm C, Axer H, Sinnreich M, Décard BF, Grimm A. Ultrasound of the nerves - An appropriate addition to nerve conduction studies to differentiate paraproteinemic neuropathies. *J Neurol Sci* 2016; **362**: 188-195 [PMID: 26944145 DOI: 10.1016/j.jns.2016.01.055]

256   **Goedee HS**, Notermans NC, Visser LH, van Asseldonk JH, Franssen H, Vrancken AFJE, Nikolakopoulos S, van den Berg LH, van der Pol WL. Neuropathy associated with immunoglobulin M monoclonal gammopathy: A combined sonographic and nerve conduction study. *Muscle Nerve* 2019; **60**: 263-270 [PMID: 31269243 DOI: 10.1002/mus.26626]

257   **Spadaro S**, Grasso S, Dres M, Fogagnolo A, Dalla Corte F, Tamburini N, Maniscalco P, Cavallesco G, Alvisi V, Stripoli T, De Camillis E, Ragazzi R, Volta CA. Point of Care Ultrasound to Identify Diaphragmatic Dysfunction after Thoracic Surgery. *Anesthesiology* 2019; **131**: 266-278 [PMID: 31166236

DOI: 10.1097/ALN.0000000000002774]

258   **Qian Z**, Yang M, Li L, Chen Y. Ultrasound assessment of diaphragmatic dysfunction as a predictor of weaning outcome from mechanical ventilation: a systematic review and meta-analysis. *BMJ Open* 2018; **8**: e021189 [PMID: 30287605 DOI: 10.1136/bmjopen-2017-021189]

259   **Yuce I**, Kahyaoglu O, Mertan P, Cavusoglu H, Aydin Y. Ultrasound-Guided Microsurgical Excision for Brachial Plexus Schwannomas: Short-Term Clinical Study. *Turk Neurosurg* 2019; **29**: 594-597 [PMID: 30875079 DOI: 10.5137/1019-5149.JTN.25575-18.3]

260   **Osorio JA**, Breshears JD, Arnaout O, Simon NG, Hastings-Robinson AM, Aleshi P, Kliot M. Ultrasound-guided percutaneous injection of methylene blue to identify nerve pathology and guide surgery. *Neurosurg Focus* 2015; **39**: E2 [PMID: 26323820 DOI: 10.3171/2015.6.FOCUS15220]

261   **Coraci D**, Giovannini S, Bernetti A, Cordenonssi JT, Erra C, Piccinini G, Padua L. Nerve ultrasound to prevent and treat iatrogenic sural nerve injury. *J Electromyogr Kinesiol* 2019; **44**: 173-174 [PMID: 30201224 DOI: 10.1016/j.jelekin.2018.08.007]

262   **Buncke G**, McCormack B, Bodor M. Ultrasound-guided carpal tunnel release using the manos CTR system. *Microsurgery* 2013; **33**: 362-366 [PMID: 23417956 DOI: 10.1002/micr.22092]

263   **Rojo-Manaute JM**, Capa-Grasa A, Chana-Rodríguez F, Perez-Mañanes R, Rodriguez-Maruri G, Sanz-Ruiz P, Muñoz-Ledesma J, Aburto-Bernardo M, Esparragoza-Cabrera L, Cerro-Gutiérrez MD, Vaquero-Martín J. Ultra-Minimally Invasive Ultrasound-Guided Carpal Tunnel Release: A Randomized Clinical Trial. *J Ultrasound Med* 2016; **35**: 1149-1157 [PMID: 27105949 DOI: 10.7863/ultra.15.07001]

264   **Joseph AE**, Leiby BM, Beckman JP. Clinical Results of Ultrasound-Guided Carpal Tunnel Release Performed by a Primary Care Sports Medicine Physician. *J Ultrasound Med* 2020; **39**: 441-452 [PMID: 31449326 DOI: 10.1002/jum.15120]

265   **Petrover D**, Silvera J, De Baere T, Vigan M, Hakimé A. Percutaneous Ultrasound-Guided Carpal Tunnel Release: Study Upon Clinical Efficacy and Safety. *Cardiovasc Intervent Radiol* 2017; **40**: 568-575 [PMID: 28028577 DOI: 10.1007/s00270-016-1545-5]

266   **Clary A**, Tyler WJ, Wetmore DZ. Abstract# 45: Ultrasound neuromodulation for the treatment of peripheral nerve compression syndromes. *Brain Stimul* 2019; **12**: e16 [DOI: 10.1016/j.brs.2018.12.052]

267   **Mandeville R**, Wali A, Park C, Groessl E, Walker FO, Cartwright MS. Cost-effectiveness of neuromuscular ultrasound in focal neuropathies. *Neurology* 2019; **92**: e2674-e2678 [PMID: 31053668 DOI: 10.1212/WNL.0000000000007602]

268   **Cartwright MS**, Griffin LP, Dowlen H, Bargoil JM, Caress JB, Li ZJ, Defranzo AJ, Wiesler ER, Tuohy CJ, Balakrishnan N, Molnar JA, Baute V, Koman LA, Poehling GG, Walker FO. A randomized trial of diagnostic ultrasound to improve outcomes in focal neuropathies. *Muscle Nerve* 2015; **52**: 746-753 [PMID: 26296394 DOI: 10.1002/mus.24884]

269   **Simon NG**. Clinical and economic arguments to support a neuromuscular ultrasound service. *Clin Neurophysiol Pract* 2019; **4**: 168-169 [PMID: 31886440 DOI: 10.1016/j.cnp.2019.06.003]

270   **Walker FO**, Alter KE, Boon AJ, Cartwright MS, Flores VH, Hobson-Webb LD, Hunt CH, Primack SJ, Shook SJ. Qualifications for practitioners of neuromuscular ultrasound: position statement of the American Association of Neuromuscular and Electrodiagnostic Medicine. *Muscle Nerve* 2010; **42**: 442-444 [PMID: 20806399 DOI: 10.1002/mus.21760]